

See discussions, stats, and author profiles for this publication at: <https://www.researchgate.net/publication/347466105>

The Geology of West Antarctica (Chapter 3)

Chapter · January 2021

CITATION

1

READS

100

1 author:



[Christine S Siddoway](#)

Colorado College

124 PUBLICATIONS 1,603 CITATIONS

SEE PROFILE

Some of the authors of this publication are also working on these related projects:



ICI-Hot Project : Ice Sheet Interaction with a Hot Geotherm in West Antarctica [View project](#)



Cryogenian continental sedimentary record for Rodinia [View project](#)

3. The Geology of West Antarctica

Christine Siddoway

3.1. Overview

The physiographic province of West Antarctica (Fig. 3-1) borders the Pacific sector of the Southern Ocean and supports the West Antarctic Ice Sheet. Unlike East Antarctica, it has no cratonic elements and consists largely of thinned continental crust of the West Antarctic rift. In geographical terms, West Antarctica is that portion of the Antarctic continent that resides primarily in the western hemisphere, seaward of the 030° W – 170° E meridian. Bounded by the Transantarctic Mountains along its interior margin, West Antarctica encompasses Marie Byrd Land, Thurston Island, and the Ellsworth Mountains block, with the Ross Embayment and Weddell Sea, which altogether comprise the West Antarctic rift province and its seaward margins (Fig. 3-2). The West Antarctic ice sheet, with its dynamic fast-flowing glacier ice streams, lies within the bounds of the rift. The Paleozoic-Mesozoic bedrock of this glaciated region crops out in coastal exposures and forms extensive subglacial bedrock, encountered in offshore dredge and drill

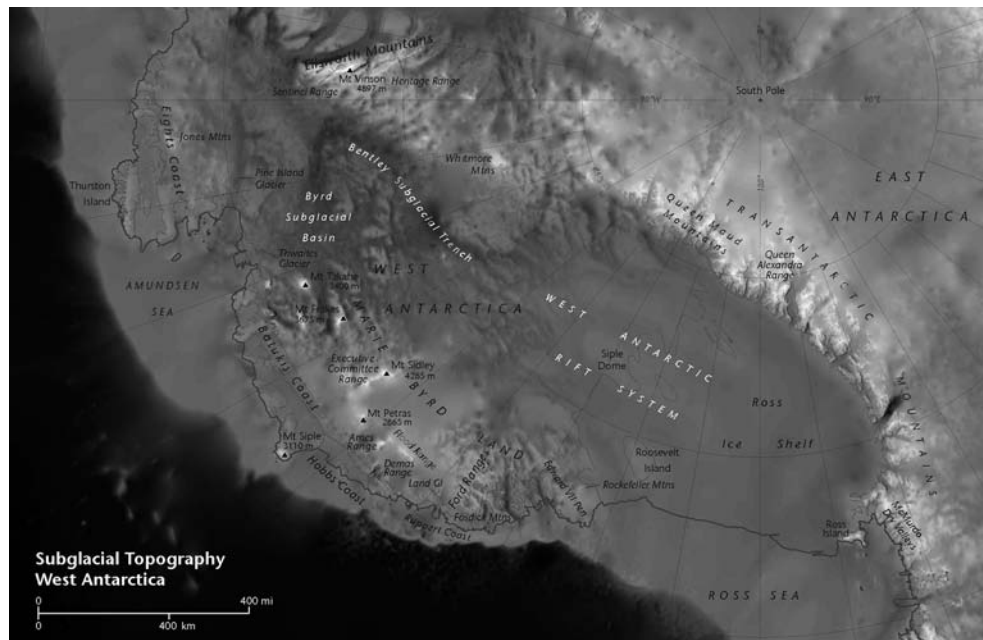


Fig. 3-1. Map of West Antarctica, showing selected place names, tectonic terranes, and physiographic features mentioned in the text. Gridded basemap is BEDMAP2 digital elevation model (Fretwell et al. 2013). Cartography by Brad Herried, Polar Geospatial Center, USA.

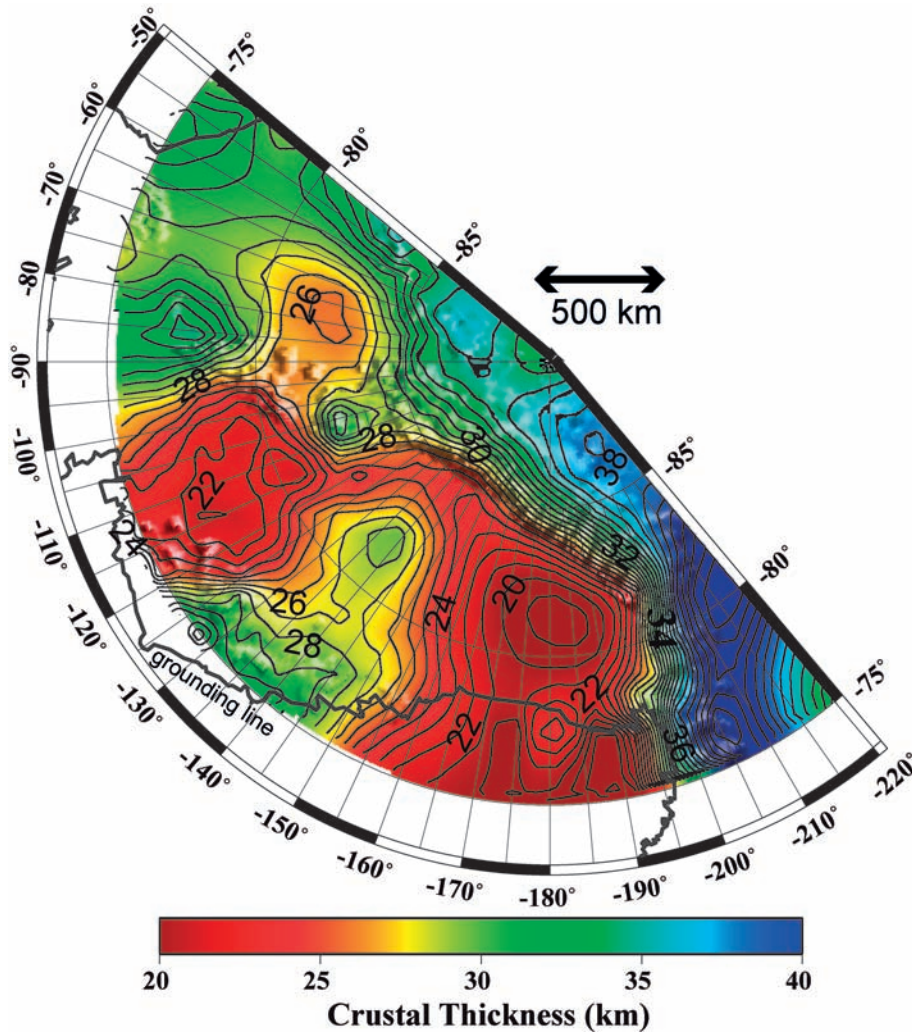


Fig. 3-2. Crustal thickness map for West Antarctica, from Chaput et al. (2014). Uses continent-scale surface wave constrained estimates of Sun et al. Thickness refers to the distance from the base of the ice sheet to the Moho, estimated using POLENET-ANET data and other seismic station constraints. Grey boxes indicate seismographic stations. **Inset** shows the demarcation of terranes in West Antarctica (Storey et al. 1988a, Randall & MacNiocaill 2004), with the oldest terranes of cratonic affinity shown in grey.

core samples. West Antarctica hosts a Neogene volcanic province that includes eruptive centers as young as Pleistocene and Holocene. Alkalic polygenetic volcanoes crown the central elevated region of Marie Byrd Land, where volcano summits reach elevations up to 4180 meters.

Formed along the Paleozoic – Mesozoic active margin of Gondwanaland, the lithosphere of West Antarctica consists of disparate Paleozoic-Mesozoic crustal blocks – tectonic terranes (Fig. 3-3) – that record the stabilization and growth of continental crust along a convergent margin, followed by intracontinental extension and wrench tectonics. The prevalent Cenozoic record is of sparse, widespread alkalic volcanism; narrow-mode

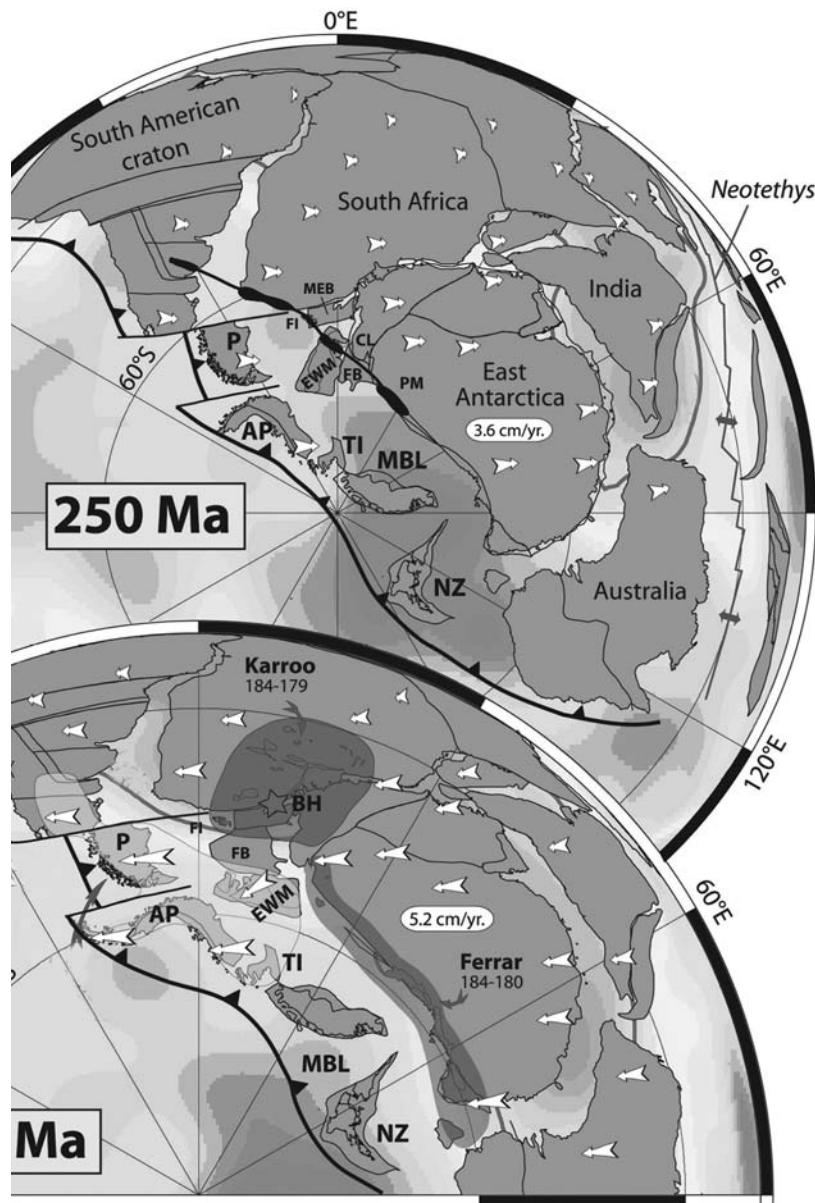


Fig. 3-3. Tectonic reconstructions showing tectonic terranes of West Antarctica within the Gondwana supercontinent and their comparative positions at a) 250 Ma and b) 180 Ma, from Torsvik et al. (2008). Terrane abbreviations are: AP: Antarctic Peninsula, EWM: Ellsworth-Whitmore, TI: Thurston Island-Eights Coast, and MBL: Marie Byrd Land. Other abbreviations are: PM: Pensacola Mountains, CL: Coats Land, FI: Falkland Islands, FB: Filchner Block, BH: Bouvet hotspot, NZ: Zealandia, P: Patagonia. The black thick line in (a) marks the location and trend of the Permian-Early Mesozoic Gondwanide orogen (Dalziel & Grunow 1992, Curtis 2001, Randall & MacNiocaill 2004), a tectonic element that links the EWM block to the Pensacola Mountains, Falkland Islands, and South Africa. The EWM block formed within the Natal Embayment in (a) and underwent at least 90° of counterclockwise rotation during supercontinent breakup. The dark grey pattern in (b) shows the extent of the Ferrar magmatism in Antarctica and Karroo magmatism in South Africa, expressions of plume activity centered upon the Bouvet hotspot at the time of breakup. Absolute plate motion vectors are denoted with white arrows and mean plate velocities for the "East Antarctic Craton" are given.

rifting from Miocene to present; and landscape rejuvenation in response to post-Pliocene focused incision by ice streams and outlet glaciers.

The terranes of West Antarctica are distinguished on tectonostratigraphic grounds and on the basis of isotopic signatures. The single known exposure of Precambrian rock, at Haag Nunataks (Fig. 3-3), is >1050 Ma. Isotopic characteristics of ultramafic xenoliths obtained from Miocene to Pleistocene volcanoes suggest a considerable extent of concealed old lithosphere. The major geological-tectonic provinces that are distinguished in West Antarctica are: the Ellsworth-Whitmore Mountains, the Ross and Amundsen provinces in Marie Byrd Land, Eights Coast-Thurston Island, the West Antarctic rift system; and the Antarctic Peninsula. Within this volume, the geology of the Antarctic Peninsula (chapter 2: Smellie, this vol.) is presented separately from that of West Antarctica. New geophysical evidence reveals the lithospheric-scale structures that form the boundaries between these crustal blocks and provinces: they correspond to deep, linear, subglacial troughs. The data also show that the Ellsworth-Whitmore Mountains block has a deep crustal root and that Marie Byrd Land is underlain by anomalous mantle characterized by slow seismic velocities, indicative of a major thermal anomaly. The margins of the Thurston Island block are delineated by gravity and magnetic anomalies indicative of recently active or active rifts.

This chapter begins with a review of the stratigraphy, geological evolution, and structural architecture of the three West Antarctica terranes (Fig. 3-2, inset) (Dalziel & Elliot 1982, Storey et al. 1988a, Storey et al. 1991) that border the West Antarctic rift province. Next it examines the geotectonic characteristics of the West Antarctic rift system, from the perspective of West Antarctica, itself, and explores the question of the genetic relationship between the West Antarctic rift system and the Transantarctic Mountains that form the rift province boundary with the East Antarctic craton. Understanding of the bedrock geology beneath the Ross Sea, the vast expanse of the West Antarctic ice sheet, and the continental shelf of the Amundsen Sea is provided by the results of airborne and marine geophysical explorations. The chapter concludes with an examination of the Marie Byrd Land volcanic province and other geological associations of special contemporary significance or scientific potential in respect to the dynamic lithosphere-cryosphere-ocean system of West Antarctica.

3.2. Ellsworth-Whitmore Mountains Terrane

Extensive rock exposures in the Sentinel and Heritage Ranges, that together comprise the Ellsworth Mountains, form the backbone of the geology of the Ellsworth-Whitmore Mountains terrane. The crustal thickness in this region (Fig. 3-2) is 32 to 37 km (Chaput et al. 2014), in dramatic contrast to adjacent crust within the West Antarctic rift province that is between ~26 and 19 km thick (Jordan et al. 2010). Recent aerogeophysical investigation of this region (Jordan et al. 2013, Ross et al. 2014) broadens the known subglacial extent of the Ellsworth-Whitmore Mountains terrane to the south and southeast, toward the TAM. Deep, narrow basins separating the tectonic blocks are interpreted to be lithospheric-scale faults having Mesozoic tectonic inheritance. The Bentley subglacial trough is the most sharply defined of these basins (Lloyd et al. 2015). The greatest topographic relief in West Antarctica occurs upon one such structure that controls the Ellsworth Mountains block margin and the position of the Rutford Ice Stream (Fig. 3-4). A vertical exchange of 7 km is achieved over a lateral distance of 40 km, from the summit of Mt. Vinson at 4892 m, to the bed of Rutford Ice Stream at -2200 m. This structural

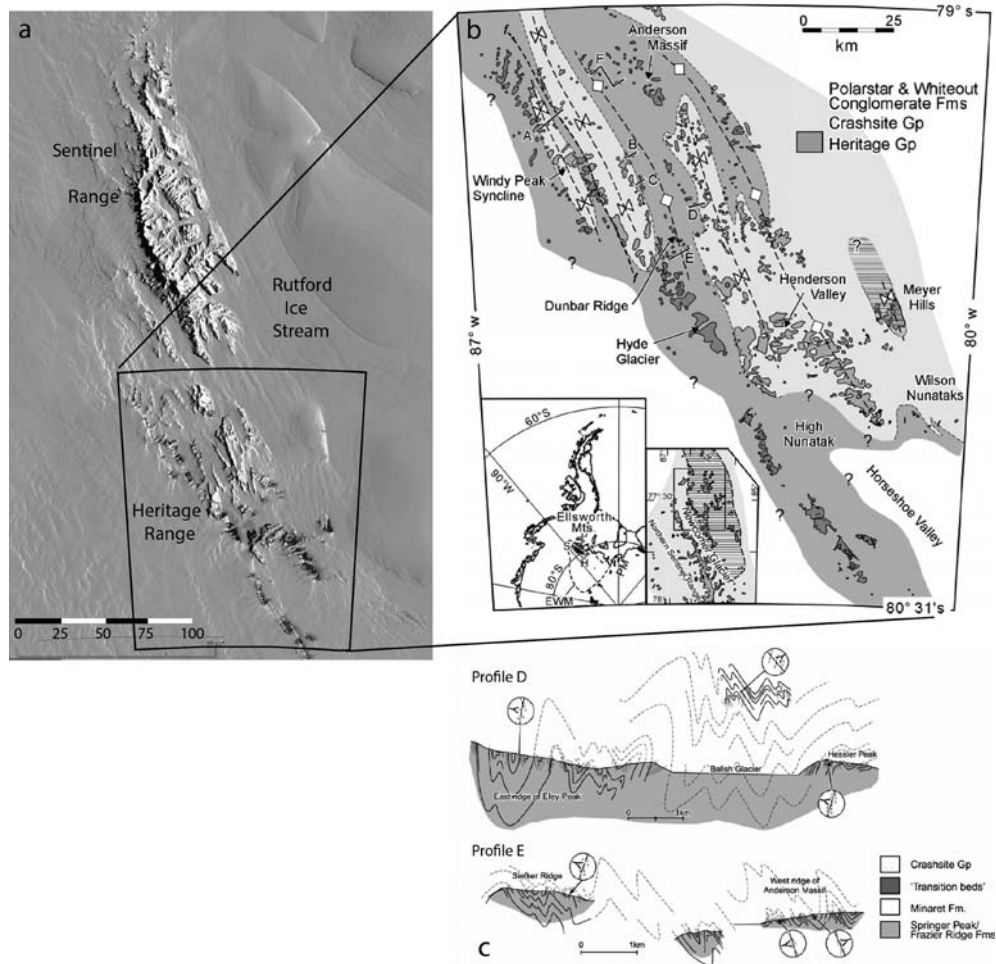


Fig. 3-4. (a) Satellite image map of the Ellsworth Mountains (GoogleEarth, DigitalGlobe, ©U.S. Geological Survey 2015a). The box outlines the area detailed in (b). (b) Structural map of the southern Ellsworth Mountains (Heritage Range), and (c) selected cross sections to illustrate the geometries of upright to steeply inclined folds, and bedding-cleavage-fault relationships in the Springer Peak Formation. From Curtis (2001). The structural cross sections are along profiles d and f, indicated on the map. The Heritage Group consists of siliciclastic sediments deposited as synrift fill in latest Early Cambrian to Late Cambrian time. The overlying Crashsite Group (Fig. 3-4) represents the transition to passive margin sedimentation. The Cambrian through Permian strata were together deformed during the Permian-Triassic Gondwanian orogeny (Fig. 3-3a).

zone separates the Ellsworth range from a tectonic microblock that hosts Haag Nunataks (). The Whitmore Mountains are an isolated group of four summits of crystalline bedrock at ~3000m elevation, located SW of the Ellsworth Mountains. The small exposures of Proterozoic gneiss forming Haag Nunataks stand above Fowler Ice Rise, east of the Heritage Range. The Haag Nunataks are distinguished as the only exposures of Precambrian rock in West Antarctica (Millar & Pankhurst 1987, Flowerdew et al. 2007).

The Ellsworth Mountains consist of a 13-km-thick succession of Paleozoic volcanic and sedimentary rocks (Fig. 3-5) deposited in active rift to passive margin settings along the margin of West Gondwana (Curtis 2001, Elliot et al. 2015 and references therein).

Early Paleozoic strata are grouped into the Early to Late Cambrian Heritage Group and Late Cambrian to Devonian Crashsite Group (Fig. 3-5). The Heritage Group (Curtis et al. 1999) is dominated by siliciclastic sediments that include lahar and ash-flow tuff deposits, fluvial to shallow marine deltaic deposits and black shales, and lesser carbonates. Basaltic volcanic and subvolcanic rocks occur at intervals, wherein there are growth faults and intraformational unconformities. Conglomerates, derived in part from contemporaneous volcanic rocks, reflect higher energy fluvial transport arising from development of topographic relief. Taken together, the characteristics indicate rapid deposition in a continental rift basin. The contact between the Heritage and Crashsite Groups marks the transition from rifted to passive margin, comparable and correlative to that recorded in Middle to Late Cambrian strata in southern Africa (Curtis 2001, Flowerdew et al. 2007), creating a sound basis for tectonostratigraphic correlation between the Ellsworth Mountains and Cape Fold Belt, Africa, in early Paleozoic time (Curtis & Storey 1996, Curtis 2001, Randall & MacNiocaill 2004, Flowerdew et al. 2007).

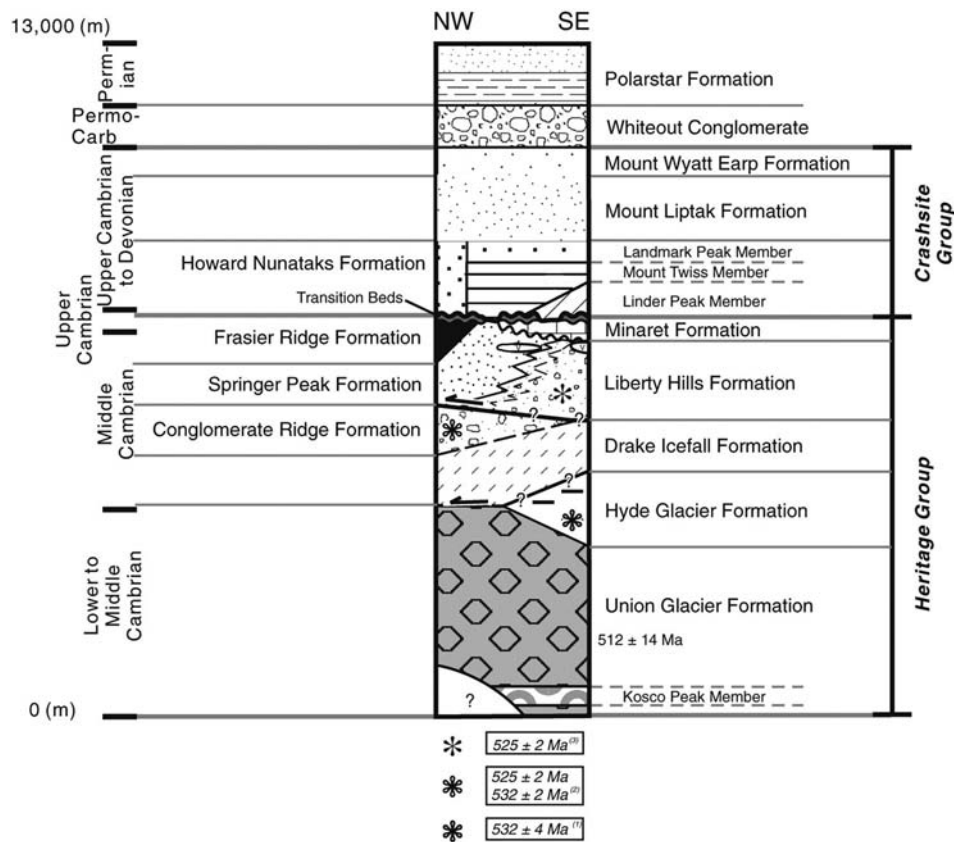


Fig. 3-5. Tectonic-stratigraphic column for the Ellsworth Mountains, from Curtis (2001) and Flowerdew et al. (2007). The depositional age of 512 Ma for Union Glacier formation is indicated. Asterisk symbols upon the column show the position of age determinations from clasts (e.g. Rees & Duebendorfer 1997), used to constrain formations' ages and reveal tectonic discontinuities. The solid lines with shear arrows correspond to major tectonic breaks with direction of tectonic transport. Wavy lines mark sequence boundaries and dashed lines are for inferred stratigraphical contacts.

The Crashsite Group (Spörli 1992) consists of 3000m of varicolored orthoquartzites and argillites accumulated in a shallow marine setting during Late Cambrian through Devonian time (Fig. 3-5). Uppermost in the Paleozoic succession are the Carboniferous to Permian Whiteout Conglomerate and Permian Polarstar Formation. The Whiteout Conglomerate (Matsch & Ojakangas 1992) is massive glacial diamictite up to 1000m in thickness, deposited during Carboniferous-Permian Gondwanide glaciation. Silicic and carbonate clasts, generated and transported by ice sheets, have East Antarctica provenance. Characteristics of some deposits indicate direct emplacement by glacier ice whereas others suggest deposition from floating ice and currents in proximity to the glacial grounding line (Matsch & Ojakangas 1992). The Polarstar Formation (Collinson et al. 1992, Elliot et al. 2015) consists of argillite in the lower part, coarsening-upward argillite to sandstone cycles with lenticular to flaser bedding in the middle, and fining-upward cross-bedded channel sandstones in the upper portion. Capping the sequence are carbonaceous strata and siltstones containing *Glossopteris* plant fossils. The formation contains abundant volcanogenic detritus, attributed to sources on the Gondwana convergent margin. New U-Pb geochronology data for igneous zircon from the ashbeds and youngest detrital grains from sandstone and argillite provide evidence that the Polarstar Formation is entirely Permian, accumulated in the interval 270 to 258 Ma (Elliot et al. 2015).

The Whitmore Mountains (Figs. 3-1, 3-3) consist of Early Jurassic Mount Seelig granite (Webers et al. 1992a) that intruded arkosic turbidite rocks; the feldspathic sedimentary rocks form a metamorphic aureole and roof pendants within the granite (Storey & Macdonald 1987). High grade assemblages occur at one locality, Mt. Woolard, where migmatitic garnet-biotite-plagioclase paragneiss and two-pyroxene amphibolite gneiss are found (Storey & Dalziel 1987). Recent investigation of U-Pb age and Hf isotope characteristics of detrital zircon from the paragneiss point to derivation from proximal sources, and a correlation to rift sediments of the Heritage Group in the Ellsworth Mountains (Flowerdew et al. 2007). High uppermost mantle velocities beneath the Whitmore region, indicative of cool, viscous, older sublithospheric mantle (Chaput et al. 2014), however, show that the Whitmore Mountains merits designation as a tectonic subprovince.

The oldest gneisses in West Antarctica crop out at Haag Nunataks, northeast of the Ellsworth Mountains. Rb-Sr whole-rock isochron ages are 1176 ± 76 Ma for the protolith, and a minimum age is provided by a crosscutting microgranite of 1058 ± 53 Ma (Millar & Pankhurst 1987). This occurrence is the single known exposure of Precambrian rocks in West Antarctica. Recent aerogeophysical surveys of this region (Jordan et al. 2013) indicate the presence of Haag-type gneisses within the Ellsworth Mountain block, and a greater extent of Proterozoic crystalline basement rocks than had been previously known.

Deformation during the Permian-Triassic Gondwanian orogeny imparted folds and cleavage upon the Cambrian to Permian strata of the Ellsworth Mountains (Fig. 3-4) (Curtis 2001, Curtis et al. 2004), and fabrics in Whitmore Mountains gneisses. The first phase of deformation, D_1 , is marked by N-S to NE-SW trending thrust faults and meso-scale folds with axial planar cleavage. D_2 deformation commenced upon bedding-parallel thrust faults, accompanied by intraformational imbrication and duplexing, and mylonitization upon faults. As deformation progressed, intense folding and a penetrative regional cleavage developed that overprinted or transposed D_1 and early D_2 structures in discrete zones, accompanied by a change from dip slip reverse to dextral transpression. Dominant NW-SE trending folds are a product of this phase (Fig. 3-4). As emphasized, Cambrian through Permian strata of the Ellsworth-Whitmore Mountains terrane are affected, making it plain that the deformation events are Permian or younger. There is a paucity of evidence of the effects of the end-Cambrian Ross Orogeny (see chapter 4: Goodge, this volume).

This lack of evidence of deformation arising from the Ross Orogeny has been much deliberated (Curtis 1998, Duebendorfer & Rees 1998, Curtis 2001 and references therein), because Middle to Late Cambrian contractional to transpressional deformation did affect other sites in this broad region (see Chapter 4: Goodge, this volume), such as the Stewart Hills, Thiel Mountains, and Pensacola Mountains, that contain potentially correlative strata (Rees & Duebendorfer 1997, Duebendorfer & Rees 1998, Curtis et al. 2004). Recent detrital zircon investigations (Flowerdew et al. 2007), however, show clear distinctions in respect to U-Pb age and Hf isotopes for the Heritage Group of the Ellsworth Mountains, compared to the other locations that share an affinity. The detrital zircon evidence, together with the correlation to the contemporaneous Middle to Late Cambrian continental rift evolution for the Cape fold belt (Curtis 2001) resolve the dilemma. The continental rifting and mafic volcanism in the Ellsworth Mountains and South African sectors of the Gondwana margin likely occurred in a back-arc or inboard setting with respect to the subduction margin (Fig. 3-3), which was undergoing extension at the same time that convergent processes along the active margin affected the rest of the Transantarctic Mountains (Curtis & Storey 1996, Rees & Duebendorfer 1997, Curtis 2001).

A later phase of intracontinental deformation during the Permo-Triassic Gondwanan orogeny (Curtis 1998) and initial stages of breakup between East and West Gondwana led to plate reorganization and the development of the Ellsworth-Whitmore Mountains as a discrete terrane. The Jurassic plutonism in the Whitmore Mountains and Pirrit Hills (Storey et al. 1988b, Lee et al. 2012), and inferred faults corresponding to well defined magnetic lineaments (Jordan et al. 2013), are expressions of the early phase of breakup in the Weddell Sea sector. Disparities in the geometry of fold-thrust structures and of paleomagnetic pole positions indicate that the Ellsworth block moved independently from South Africa and East Antarctica, and underwent a *ca* 90° anticlockwise rotation with respect to its original position along the Gondwana margin (Fig. 3-3), and contemporaneous units in the Transantarctic and Pensacola Mountains (Dalziel et al. 1987, Grunow et al. 1987, Randall & MacNiocaill 2004). Some amount of lateral translation for the block is called upon to explain the absence, in the Ellsworth Mountains, of the effects of deformation and magmatism that occurred in the Transantarctic and Pensacola Mountains, to which the Ellsworth Mountains restore (Curtis 2001; chapter 4: Goodge, this volume). The kinematics and amount of lateral translation is debated, however (Grunow et al. 1987, Curtis et al. 1999, Randall & MacNiocaill 2004, Jordan et al. 2013). It is possible that the newly recognized wrench systems bounding the Ellsworth-Whitmore Mountains terrane (Jordan et al. 2013) accommodated this displacement, however this interpretation is difficult to test directly due to the cover of the Antarctic ice sheet. According to results from apatite fission-track analysis of samples from a 4.2-kilometer vertical transect upon the west side of the Vinson Massif (Fitzgerald & Stump 1991), bedrock uplift in the Ellsworth Mountains commenced after the initial separation of East and West Gondwana and coincided with the opening of the Weddell Sea in the Early Cretaceous Period (Fitzgerald & Stump 1991, Fitzgerald & Stump 1992). Mountain relief has been sustained in the Ellsworth Mountains since that time.

3.3. Marie Byrd Land

Marie Byrd Land is a product of the Paleozoic and Mesozoic convergent accretionary margin of East Gondwana (Figs. 3-3, 3-6) (i.e. Collins 2002). The terrain contains the most complete record of the growth and stabilization of the new continental crust of West

Antarctica (Antarctic Peninsula, excluded: see Chapter 2 of this volume for an overview of the development of the Antarctic Peninsula terrane) provided by four principal rock associations. The geological associations are: 1) Cambrian–Ordovician turbiditic sedimentary rocks, several kilometres in thickness (Fig. 3-7a) (Bradshaw et al. 1983, Adams 1986), 2) Paleozoic calc-alkaline metaluminous to peraluminous plutonic rocks (Fig. 3-7b) (Weaver et al. 1991, Pankhurst et al. 1993, Pankhurst et al. 1998, Mukasa & Dalziel 2000, Siddoway & Fanning 2009, Yakymchuk et al. 2015), 3) migmatite-granite complexes that represent exhumed middle crust (Fig. 3-7c) (Richard et al. 1994, Smith 1996, Mukasa & Dalziel 2000, Siddoway et al. 2004b, McFadden et al. 2010a, McFadden et al. 2010b, Korhonen et al. 2010a, Korhonen et al. 2010b); and 4) Mesozoic-dominantly Cretaceous-alkalic to calc-alkaline granites and mafic dikes (Fig. 3-7d) (Weaver et al.

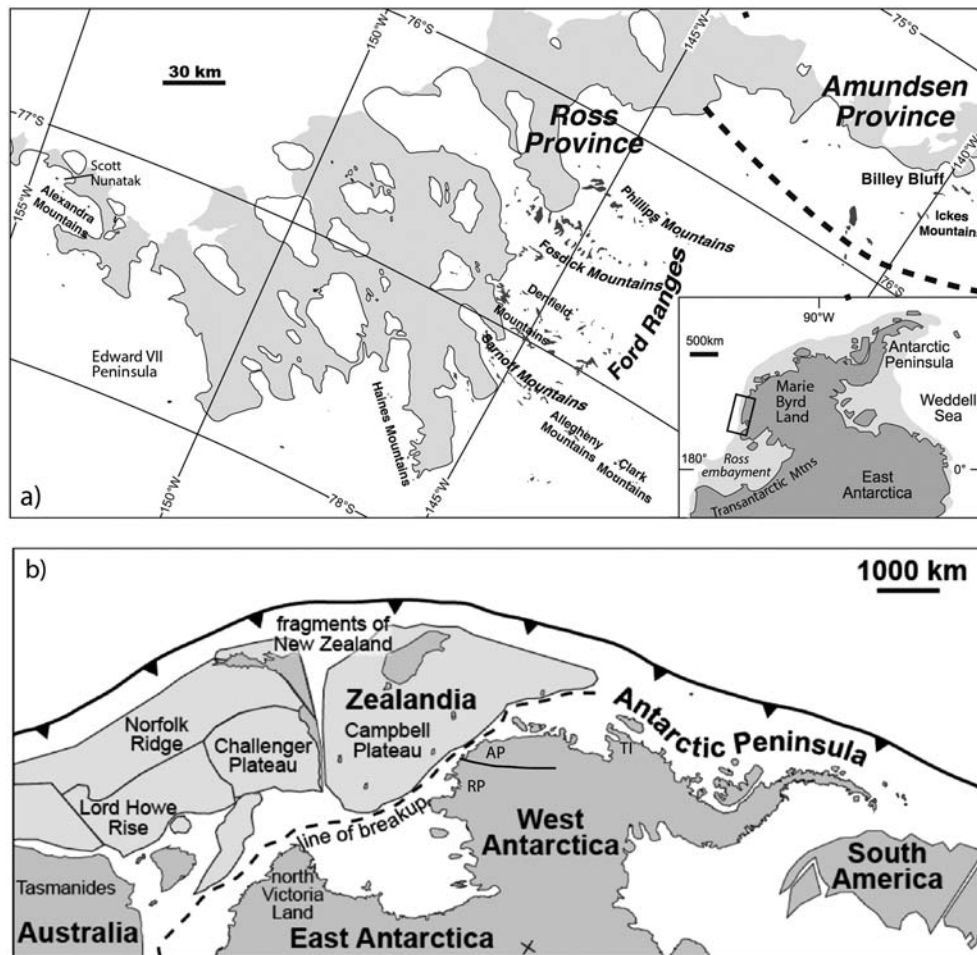


Fig. 3-6. (a) Geographic map of the Ford Ranges in western Marie Byrd Land, with locations of features mentioned in the text. The inferred boundary between the Ross Province and Amundsen provinces is as identified by Pankhurst et al. (1998). (b) Tectonic reconstruction of the Cretaceous convergent margin East Gondwana, from Yakymchuk et al. (2015); drawing upon elements rendered in Eagles et al. (2004), Mortimer et al. (2006), and Veevers (2012). Abbreviations are RP: Ross Province, AP: Amundsen Province, and TI: Thurston Island terrane.

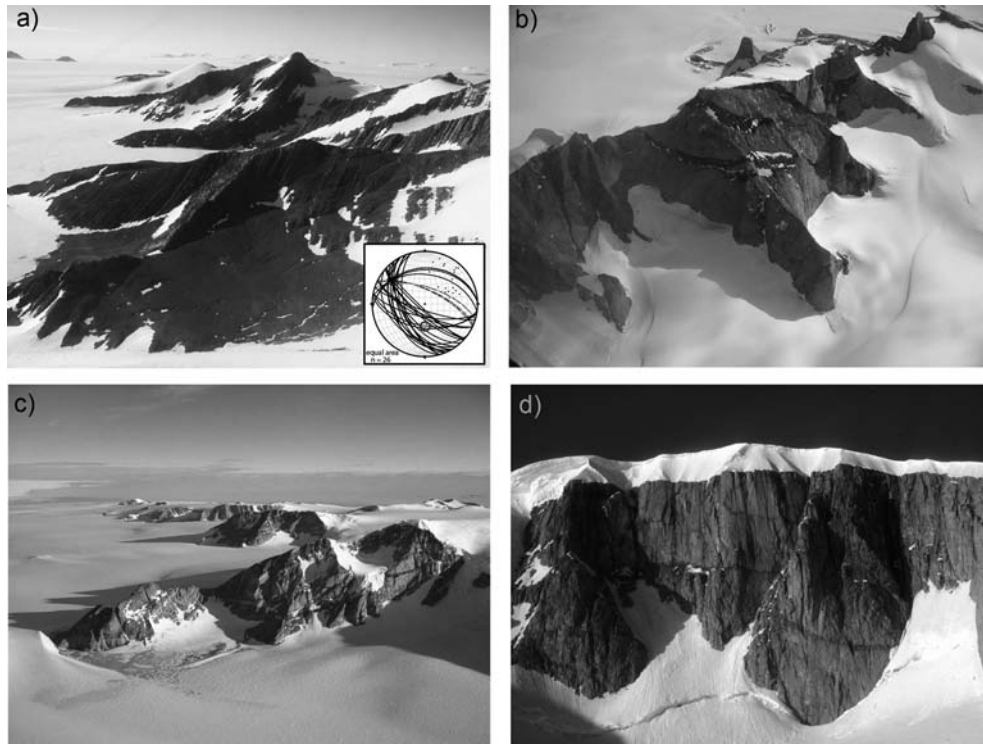


Fig. 3-7. Photographs illustrating the principal rock formations of Marie Byrd Land. (a) Dark-colored turbidite sedimentary rocks of the Swanson Formation, along-strike view along the northeast-dipping limb of a steep, upright fold. Strata are metamorphosed to lower greenschist grade, associated with development of axial planar cleavage and quartz veins (Photo: C. Yakymchuk). Inset is an equal area stereographic plot of planes of Swanson Formation bedding (solid lines) and average planes of cleavage (dashed lines) corresponding to NW-SE oriented symmetrical tight upright folds. (b) Phaneritic, unfoliated main phase of the Ford Granodiorite suite, containing dark roof pendants of Swanson Formation, southern Ford Ranges. (c) Granite-migmatite association of the Fosdick Mountains gneiss dome, view to east along the north flank of the Fosdick range. (d) Byrd Coast Granite, Bowman Peak, Edward VII Peninsula.

1991, Weaver et al. 1994, Adams et al. 1995, Mukasa & Dalziel 2000, Siddoway et al. 2005, Saito et al. 2012, Yakymchuk et al. 2013). The most extensive rock exposures of these units are in the Ford Ranges of western Marie Byrd Land (Fig. 3-1).

As a consequence of distinctions in bedrock units, timing of plutonism, Nd model ages, and paleomagnetic characteristics, Marie Byrd Land is divided into two tectonic provinces (Fig. 3-6). The Ross Province consists of voluminous Cambrian turbidites and flysch of the Swanson Formation, intruded by 375–345 Ma calc-alkaline granitoids of the Ford Plutonic suite that have Nd model ages of 1.5–1.3 Ga (Pankhurst et al. 1998). Detrital zircon U-Pb age distributions from Swanson Formation and metamorphosed equivalents contain a significant age component of ca. 1.2–1.0 Ga (Yakymchuk 2014, p. 174). The Amundsen Province consists of plutonic rocks of Ordovician–Silurian (450–420 Ma) and Permian–Triassic age, that yield younger Nd model ages of 1.3–1.1 Ga (Pankhurst et al. 1993, Pankhurst et al. 1998); sedimentary rocks are lacking. Both provinces host Cretaceous calcalkaline to alkaline plutonic rocks (Weaver et al. 1991, McFadden et al. 2010a, Yakymchuk et al. 2013, Brown et al. 2016) and Miocene to Present mafic alkalic volcanoes (LeMasurier & Rocchi 2005, LeMasurier et al. 2011). Based on limited evidence

from Re–Os isotopic investigation of lherzolite and harzburgite xenoliths from young volcanoes, central Marie Byrd Land appears to be underlain by Amundsen Province-type crust: Re–Os model ages for lithosphere stabilization are ca. 1.1 to >1.3 Ga (Handler et al. 2003), consistent with Proterozoic Nd model ages obtained for Marie Byrd Land granites and orthogneisses (Pankhurst et al. 1998). Paleomagnetic observations support the presence of a tectonic boundary between the two distinct provinces (DiVenere et al. 1996, Luyendyk et al. 1996), in the vicinity of Land Glacier (Fig. 3-1), however the orientation is unknown due to the extensive ice cover and the lack of geophysical data in that area.

3.3.1. Ross Province

The oldest exposed rocks in the Ross Province are the Swanson Formation, voluminous Cambrian–Ordovician turbidites and flysch (Fig. 3-7a) of the type that dominates the sedimentary record of Gondwana’s proto-Pacific margin (Figs. 3-3, 3-6). The source of the voluminous sediments of East Gondwana was the Ross–Delamerian orogen (Ireland et al. 1994, Adams et al. 2005, Adams et al. 2014; chapter 4: Goodge, this volume). The Swanson Formation is intruded by 375–345 Ma calc-alkaline, I-type plutons and associated granites that comprise the Ford Plutonic Suite (Fig. 3-7b) (Pankhurst et al. 1998, Siddoway & Fanning 2009, Yakymchuk et al. 2015) and by Cretaceous alkali granites of circa 115 to 97 Ma (Fig. 3-7c) (zircon U–Pb ages: Siddoway et al. 2004a, McFadden et al. 2010a, Yakymchuk et al. 2013). These occur as plutons intruding Swanson Formation and Ford intrusives, and as stacked, thick sills and discordant dikes in the Fosdick Mountains. The Ross Province appears to extend at least as far south as Roosevelt Island and Siple Dome, based on the presence of 370–330 Ma (Ford suite provenance) and 110–100 Ma (derived from Cretaceous arc or A-type magmatic rocks) U–Pb age populations in detrital zircon sampled from sub-ice stream sediment-age groups that are absent from subglacial tills of East Antarctic ice streams (Licht et al. 2014).

Detrital zircon provenance is central to the understanding of sediment transport and tectonic relationships for the Gondwana margin in early Paleozoic time. Swanson Formation and its correlatives in Australia (Lachlan Group), northern Victoria Land (Robertson Bay Group), and New Zealand (Greenland Group) represent sedimentary detritus eroded from and accumulated outboard of the Cambrian Delamerian–Ross Orogen (Flöttmann & Kleinschmidt 1993, Ireland 1992, Ireland et al. 1994, Ireland et al. 1998, Adams 2004, Veevers & Saeed 2011; chapter 4: Goodge, this volume). The regionally extensive greywackes contain some common detrital zircon U–Pb age populations of ca. 650–490 Ma and ca. 1.2–1.0 Ga, and a scattering of small Archean age groups (e.g. Adams et al. 2014, Hawkesworth & Kemp 2006). New Hf and O isotope analyses for detrital zircon from Swanson Formation and equivalent metasedimentary rocks allow the interpretation of provenance to be refined (Fig. 3-8, Yakymchuk et al. 2015). Three principal age populations in western Marie Byrd Land include Neoproterozoic–Cambrian zircons with evolved Hf isotope values that indicate derivation from reworked Mesoproterozoic crust, interpreted to be igneous and metamorphic rocks of the Ross–Delamerian Orogen; Mesoproterozoic detrital zircons with juvenile Hf isotope values that are consistent with derivation from crust resembling the gneiss of Haag Nunataks (Fig. 3-8; see section 3.2., above) or a sedimentary derivative Haag-type crust that is concealed beneath the Antarctic ice sheet; and Paleoproterozoic zircons sourced from crystalline basement of the sort that is exposed in the central Transantarctic Mountains (Yakymchuk et al. 2015). All are of continental derivation (e.g. Glen 2005, **Gelen** 2013).

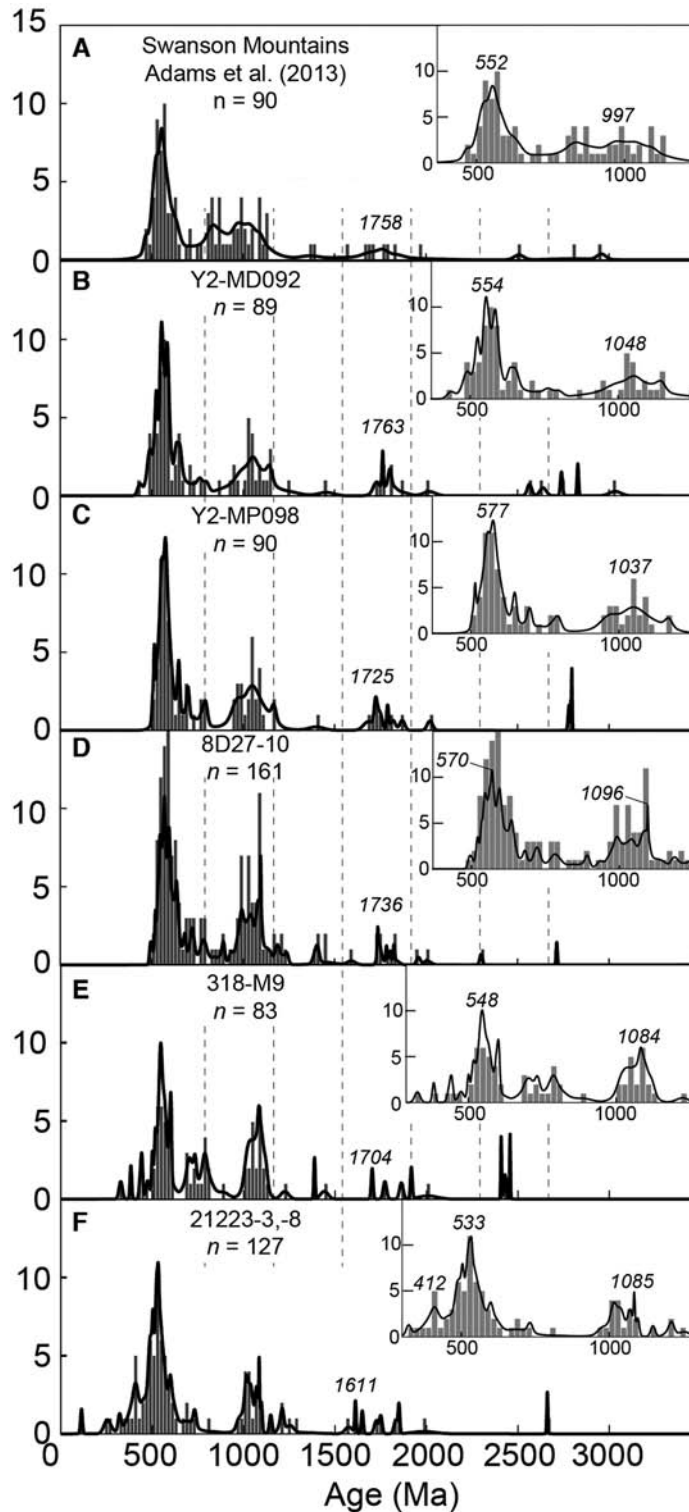


Fig. 3-8. Histograms and normalized probability distribution curves (inset) of detrital zircon U-Pb ages obtained from Swanson Formation (A–C) and metasedimentary rocks (D–G) of western Marie Byrd Land. Diagram is from Yakymchuk et al. (2015).

A current model for formation of the thick turbidites of the Australian Tasmanides, the Lachlan Group, involves deposition as submarine fan complexes in a back-arc or marginal oceanic basin, followed by tectonic imbrication, thickening, and low grade metamorphism due to accretion to the continental margin (Foster et al. 2009, Glen 2013). As for the Lachlan, so was the succession of events for the immature sedimentary strata in other sectors of Gondwana's active margin, albeit during different intervals of early Paleozoic time. In the Ross Province, folding and low greenschist grade metamorphism affected the Swanson Formation in the Late Ordovician, between 450–421 Ma (Adams 1986, Adams et al. 1995, Kleinschmidt & Petschick 2003). Kilometres-scale upright folds and cleavage in the Swanson Formation trend NW-SE, and folds plunge gently to the NW (Fig. 3-7a) (Wade & Couch 1982, Siddoway & Fanning 2009). If the Tasmanides model applies broadly to the Gondwana margin and Ross Province, then the cleavage development and folding of Swanson Formation reflects accretion and telescoping of the Ross Province of Marie Byrd Land during Paleozoic plate convergence along the Gondwana margin (Boger 2011).

Calc-alkaline, primarily I-type plutonism became established in the Ross Province from 375–345 Ma, in the latest Devonian to Carboniferous (Pankhurst et al. 1998, Siddoway & Fanning 2009, Yakymchuk et al. 2015). The intrusives form the Ford Granodiorite suite (Fig. 3-7b) and are a product of convergent margin arc magmatism (Weaver et al. 1991, Pankhurst et al. 1998, Yakymchuk et al. 2015) that was widespread in East Gondwana (Tulloch et al. 2009, Borg et al. 1986, Borg et al. 1987, Fioretti et al. 1997a, Fioretti et al. 1997b, Chappell et al. 1988). Hf and O isotope compositions of zircons from the Ford Granodiorite record the mixing of a juvenile magma with melts derived from Swanson Formation, and an increase in the Swanson-derived component in younger members of the Ford Suite (Yakymchuk et al. 2015). Somewhat elevated ^{18}O values of zircons from Ford Granodiorite are attributed to the Swanson metasedimentary components that were subjected to surface processes such as weathering and sediment transport (e.g. Hawkesworth & Kemp 2006).

Consistent with the geochemical and isotopic evidence for crustal melting of the Swanson Formation, mid-crustal exposures of in the Fosdick Mountains (Fig. 3-7c) consist of migmatitic paragneiss derived from Swanson Formation (Siddoway et al. 2004b, Yakymchuk 2014). Peak conditions at ca. 360 Ma entailed temperatures in excess of 800 °C, and pressure $P > 750$ MPa (7.5 kbar) (Fig. 3-9a) (Korhonen et al. 2010b, Yakymchuk 2014), corresponding to crustal depths of 25 km or greater. Metasedimentary rock protolith compositions yielded melt volumes up to 25%. Under sustained high temperature conditions within the Fosdick complex, anatexis of the Devonian granodiorites in the mid-crust (early Ford Granodiorite suite) also occurred, producing 2 to 10 volume per cent melt from the breakdown of hornblende and plagioclase at temperatures above biotite stability (Korhonen et al. 2010a, Korhonen et al. 2010b). Material derived from both sources surpassed the melt connectivity transition of ~7 vol.%, leading to development of melt extraction pathways and melt loss from the midcrustal source region (Fig. 3-9a). Peraluminous granites of ca. 330 Ma in the Ford Ranges are possible derivatives of the crustal melting (Pankhurst et al. 1998, Korhonen et al. 2010b, Brown et al. 2016).

The temporal trend in source compositions in Paleozoic plutonic rocks in the Ford Ranges indicates an advancing or neutral accretion mode along the Gondwana convergent margin in Marie Byrd Land (Yakymchuk et al. 2015) that contrasts with the rapid extension mode documented in same-aged granitoids in Western Province of New Zealand (Tulloch et al. 2009).

uncorrected proofs

14

3. The Geology of West Antarctica

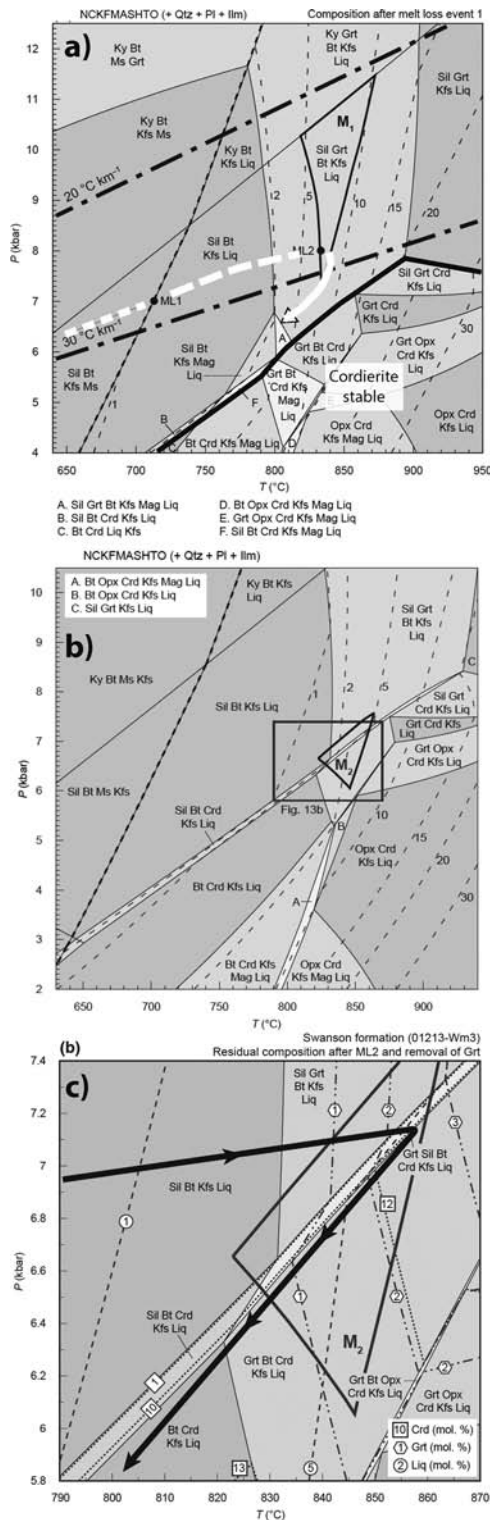


Fig. 3-9. Pressure-temperature (P-T) conditions for regional metamorphism in Marie Byrd Land, based on mid-crustal exposures of the Fosdick Mountains migmatite-granite complex, exhumed during Cretaceous detachment faulting and gneiss dome formation (McFadden et al. 2010a). P-T pseudosections are from Korhonen et al. (2011). The thin dashed lines are melt isopleths in mol.% (~vol.%); the thick dashed lines represent the solidi. Over the course of the model run for melt loss, the solid shift to higher temperatures because compositions become more residual due to melt loss. (a) Pseudosection used to characterize M1, regional metamorphism affecting western Marie Byrd Land during Devonian–Carboniferous plate convergence and orogenic I-type magmatism. Bulk composition for the sedimentary protolith was established from whole rock analyses of representative Swanson Formation samples. The prograde path (dotted line) within the sillimanite field is based on petrological evidence (Korhonen et al. 2010b). Melt-loss events ML1 and ML2 (black circles) correspond to points of modeled melt production of 7 mol.% (~vol.%). (b) Pseudosection calculated for Cretaceous high temperature metamorphism (M2), modeled on the basis of representative Swanson Formation composition modified by Devonian–Carboniferous melt loss, M1. The bold line delimits the peak field for M2 metamorphism, and the box denotes the pseudosection detail in Fig. 3-9c. (c) Expanded area from (b), contoured for mol.% melt, garnet and cordierite. The interpreted Cretaceous P–T path is shown by the heavy solid line.

Subsequent to the Paleozoic convergent margin, there is a gap in the geological record in Marie Byrd Land between 320 Ma (Mukasa & Dalziel 2000, Pankhurst et al. 1998) and 143 Ma, when calc-alkaline magmatism recommenced (Adams 1987, Weaver et al. 1991, Weaver et al. 1992). In the neighboring Thurston Island/Eights Coast terrane, there is a fuller record of Mesozoic magmatism (Riley et al. 2017b), that is summarized below. Contemporaneous I-type magmatism, with emplacement of leucogranite to monzogranite occurred across both tectonic provinces of Marie Byrd Land (Pankhurst et al. 1993, Mukasa & Dalziel 2000), linked to subduction of the Phoenix oceanic plate and possibly other oceanic microplates (Sutherland & Hollis 2001, Seton et al. 2012, Wobbe et al. 2014). Geochemical characteristics, including pronounced negative Nb anomalies and large-ion lithophile element abundances, support the association to subduction (Pankhurst et al. 1993, Weaver et al. 1994, Mukasa & Dalziel 2000).

In the Ross Province (Fig. 3-6) in middle Cretaceous time, regional A-type plutonism succeeded arc-related I-type activity, leading to emplacement of the Byrd Coast granite suite in western Marie Byrd Land (Adams 1987, Weaver et al. 1991, Weaver et al. 1995, Brown et al. 2016). A-type granites (Whalen et al. 1987) have distinctive geochemistry in respect to major elements (for example, high SiO_2 and $\text{Na}_2\text{O}+\text{K}_2\text{O}$; low CaO and Sr), discriminants such as Y, Nb, and Ce, and ratios of Ga/Al and Fe/Mg. The isotopic and geochemical characteristics reflect the derivation of A-type granites from partial melting of an enriched granulitic lower crust that is a residual of orogenic I-type magmatism. A-type granites commonly occur within the tectonic context of intracontinental extension, and such is the case for the Byrd Coast Granite (Fig. 3-7d) (Siddoway et al. 2004a, Siddoway 2008, McFadden et al. 2015).

The main phase of Byrd Coast Granite plutonism occurred from 115 to 95 Ma, determined from U-Pb zircon geochronology (Siddoway et al. 2004a, McFadden et al. 2010b, Yakymchuk et al. 2013, Brown et al. 2016) and whole rock Rb-Sr isochron ages (Adams 1987), for sites in the Ford Ranges and Edward VII Peninsula. On the basis of aeromagnetic evidence Byrd Coast Granite plutons are interpreted to exist in the subglacial environment (Ferriaccioli et al. 2002, Luyendyk et al. 2003). Active tectonism is recorded along the entirety of the margin of the proto-Pacific Ocean, during this interval of the Cretaceous Period, in Antarctica (Siddoway 2008, Vaughan et al. 2012), in Zealandia (Weaver et al. 1992, Muir et al. 1995, Waight et al. 1998), in Patagonia (Hervé et al. 2007), and along the North American Cordillera (Paterson & Ducea 2015). Regionally, emplacement of alkalic mafic dykes overlapped in time with Byrd Coast Granite plutonism (Siddoway et al. 2005, Saito et al. 2012), as did mid-crustal anatexis leading to gneiss dome emplacement in the footwall of the Fosdick Mountains detachment zone (see below).

In the case of mid-Cretaceous A-type plutonism in Ross province, there is strong direct evidence for renewed melting of lower middle crust, at granulite facies conditions (Korhonen et al. 2010a, Korhonen et al. 2010b, Korhonen et al. 2011, Brown et al. 2016). K-feldspar rich anatectic granites within the Fosdick Mountains have Sr, Nd, Hf and O isotope values consistent with derivation from Ford Granodiorite suite and meta-Swanson Formation represented by residual migmatite gneisses in the Fosdick complex (Yakymchuk et al. 2013, Brown et al. 2016) that experienced $T > 800^\circ\text{C}$ at $P \sim 700$ MPa (7.0 kbar) (Figs. 3-9b, 3-9c). Cretaceous anatectic granites within the gneiss dome display cumulate structures, and have variable major oxide and trace element concentrations, with low ΣREE contents and common positive Eu anomalies (Brown et al. 2016). They are interpreted as evidence of fractional crystallization and the accumulation of early-crystallized feldspar and quartz within intrusions within the source and transfer

zone, that are genetically linked to Byrd Coast intrusions at higher crustal levels in the Ford Ranges (Brown et al. 2016). Dolerite dikes of the Ross province give a wider range of ages from 142 to 96 Ma (Siddoway et al. 2005, Saito et al. 2012), with oldest dike ages matched by an early phase of Byrd Coast alkalic granite that is ca. 142 Ma in the Allegheny Mountains and ca. 131 Ma at Mt. Corey (Fig. 3-6a) (Adams 1987). Byrd Coast Granite elsewhere in the Ford Ranges gives ages of ca. 105–103 Ma and ca. 99 Ma (Richard et al. 1994, Yakymchuk 2014), and in Edward VII Peninsula is 103–98 Ma in age (Mukasa & Dalziel 2000, Siddoway et al. 2004a). The plutonism coincided with transtension to extension during a transition from oblique convergence to oblique extension occurred along the Cretaceous East Gondwana plate margin (Siddoway et al. 2004a, Siddoway et al. 2005, McFadden et al. 2010a, McFadden et al. 2010b, McFadden et al. 2015), possibly induced in part by oceanic ridge-trench interaction (Bradshaw 1989, Weaver et al. 1994, Luyendyk 1995).

This generation of alkalic dikes and syeno-granites was emplaced over a wide region of the Amundsen Province, also (Mukasa & Dalziel 2000, Weaver et al. 1994, Wandres & Bradshaw 2005). Timing is established from a dolerite dike swarm emplaced at 107 ± 5 Ma, followed closely by 102–95 Ma syenite and alkalic granite (Storey et al. 1999), marking the rapid change to transtension- and rift-related alkalic magmatism.

3.3.2. Amundsen Province

The Amundsen Province of central and eastern Marie Byrd Land (Pankhurst et al. 1998) contains a record of Ordovician-Silurian (450–420 Ma) and Permo-Triassic plutonism, comparable in timing to that of Thurston Island (see below) and the Antarctic Peninsula (chapter 2, Smellie: this volume). Sedimentary precursors are found in the form of paragneiss. The gneisses of central versus easternmost Marie Byrd Land yield distinctive populations of detrital zircons, with respect to U-Pb age range and abundance. The central region yields ages of 270 to 400 Ma (Patton Bluff and Mt. Petras), whereas the basement rocks underlying the late Miocene Mt. Murphy stratovolcano (Fig. 3-1) range from circa 480 to 1000 Ma (Fig. 3-10; Pankhurst et al. 1998). The biotite-muscovite paragneiss and granodiorite orthogneiss at Mt. Murphy are the oldest known constituents of the Amundsen Province. The U-Pb zircon emplacement age for the plutonic precursor of the orthogneiss is 505 ± 5 Ma, and Nd isotope model ages of 1.3 to 1.1 Ga indicate the presence of a Precambrian lithosphere at depth (Pankhurst et al. 1998). The isotope ages and geological history of the Amundsen Province contrast with Thurston Island, to the east (see below). Deep, narrow subglacial troughs, occupied by ice streams, separate the terranes (Jordan et al. 2010).

The single macrofossil occurrence in Marie Byrd Land comes from the Amundsen Province. Considered to be late Devonian in age, the fossils are plant impressions and carbonized plant remains, found within glacial erratics of meta-argillite that were deposited upon a granite nunatak, Milan Rock, along a headward segment of Land Glacier (Grindley et al. 1980). The erratics consist of dark carbonaceous slaty argillite, ascribed to a freshwater deltaic environment, that was tentatively assigned to the Swanson Formation (Grindley et al. 1980). The recognition of fossil material from the lycopsid *Haskinsia colophylla*, of Middle Devonian age (Xu & Berry 2008), places the correlation of the meta-argillite in question, because ~~pre-late~~ Swanson **Formatoin** is **pre-late** Ordovician (Adams 1986, Kleinschmidt & Petschick 2003).

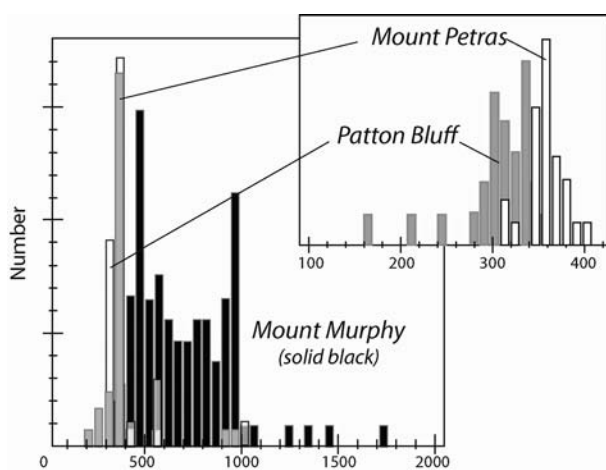


Fig. 3-10. Summary diagram showing detrital zircon age histograms of SHRIMP ^{238}U - ^{206}Pb data for paragneisses of the central and eastern Amundsen Province, from Pankhurst et al. (1998). The localities sampled in the central Amundsen Province are Mt. Petras (solid white) and Patton Bluff (solid grey). The two sites display a great deal of overlap in age; an expanded scale is therefore shown in the inset for those two samples. Mt. Murphy (Fig. 3-1) yields detrital zircon age results (solid black pattern) that are utterly dissimilar from the other Amundsen province samples, but similar to the U-Pb ages and abundance of detrital zircons in the Swanson Formation (Fig. 3-8).

Permian-aged arc intrusives (276 ± 2 Ma) underlie the Kohler Range, providing evidence of longstanding convergence along the Gondwana margin (Pankhurst et al. 1998). Their geochemistry is adakitic, suggesting derivation by melting of the subducted basaltic oceanic crust (Castillo 2006). The magmatic system is a potential source of volcanic detritus now found within the Beacon Supergroup of the Transantarctic Mountains (chapter 4: Goodge, this volume) and Crashsite Quartzite of the Sentinel Range (see above). If true, the Marie Byrd Land terrane was in proximity to East Antarctica by Permian time. A province boundary between eastern and western Marie Byrd Land (Ross and Amundsen provinces; see Fig. 3-6) is inferred on paleomagnetic grounds between the Ross and Amundsen provinces (DiVenere et al. 1996), but the region is nearly completely glaciated and there is an absence of airborne or marine geophysical data that could reveal the position of the province boundary. The boundary is expected to have a clear expression in the gravity and/or magnetic anomalies, judging from the situation for comparable features imaged in the Ford Ranges (Luyendyk et al. 2003). Restoration of the dextral component motion along the Cretaceous plate boundary (e.g. Sutherland & Hollis 2001) potentially would place the Mesozoic magmatic arc of the Amundsen province and Thurston Island outboard of the Ford Ranges (Mortimer et al. 2006, Kipf et al. 2012).

The Amundsen province and Thurston Island terranes both record plate convergence and calc-alkaline plutonism from 124–110 Ma, arising from subduction of oceanic crust (Storey et al. 1991, Pankhurst et al. 1998, Mukasa & Dalziel 2000, Riley et al. 2017b). Rock types span a range of compositions from hornblende-biotite granodiorite to monzogranite. Plutons in central to eastern MBL are calcalkaline through adakitic arc rocks, based on trace element criteria (Pankhurst et al. 1998). Anatectic granites from a migmatite-granite association in the Demas Range yielded conventional U–Pb zircon lower intercept ages of ca. 127–128 Ma and 118 to 113 Ma. Onset of A-type plutonism in the Amundsen Province is believed to be diachronous, arising at 102 Ma in the

west, near Land Glacier (Yakymchuk et al. 2015), and commencing at 96–94 Ma in the east (Mukasa & Dalziel 2000). Further east in the Thurston Island terrane, calc-alkaline magmatism continued during the same interval of ca. 96 Ma to 94 Ma, then ceased (Mukasa & Dalziel 2000, Riley et al. 2017b). Intermediate to mafic plutonic rocks are the prevalent constituents of the rock exposed at Bear Peninsula in easternmost MBL, but andesitic breccia also occurs (Pankhurst 1990, Pankhurst et al. 1998). Bear Peninsula is separated from the next terrane to the east, the Thurston Island terrane, by the deep narrow lineaments in the subglacial topography beneath the Pine Island and Thwaites ice streams (Holt et al. 2006, Vaughan et al. 2006).

On the basis of granitoid petrogenesis and ages, the Amundsen Province displays an affinity to the Takaka terrane and Median Tectonic Zone of Zealandia (Bradshaw et al. 1997, Pankhurst et al. 1998, Tulloch et al. 2009). Adakitic granites, which may be generated by melting of young subducted lithosphere, are found not only in the Amundsen Province but in New Zealand in Cretaceous time (Muir et al. 1995, Wandres et al. 1998, Allibone & Tulloch 2004) and lend support to the interpretation that the Phoenix-Pacific spreading ridge (Bradshaw 1989, Luyendyk 1995) and/or Hikurangi Plateau igneous province (Storey et al. 1999, Mortimer et al. 2006, Kipf et al. 2014) encroached on the Cretaceous subduction margin of Gondwana in this sector leading to plate reorganization.

3.3.3. Fosdick Mountains migmatite-granite complex and gneiss dome

Singular access to areally extensive exposures of migmatite and granite, representative of the lower middle and middle crust of the Ross Province, exists in the Fosdick Mountains of the northern Ford Ranges (Figs. 3-1, 3-6a). The Fosdick range is a migmatite-granite complex forming a gneiss dome, as was recognized by Wilbanks originally (1972). The elongate, 80 x 15 km structure is delimited on the south by a S-dipping, dextral-oblique detachment zone (McFadden et al. 2010b) and by an inferred steep, dextral strike-slip zone on the north (Siddoway et al. 2005, McFadden et al. 2010a) (Fig. 3-11). Field- and laboratory-based research of the migmatite-granite complex in the Fosdick Mountains has led to advances in understanding of: **a)** the differentiation and stabilization of the continental crust of Marie Byrd Land (Siddoway & Fanning 2009, Korhonen et al. 2010a, Korhonen et al. 2010b, Korhonen et al. 2011, Brown et al. 2011, Yakymchuk et al. 2013, Yakymchuk et al. 2015, Brown et al. 2016), and **b)** the kinematics, timing, and duration of tectonic exhumation of the migmatite-granite association within a Cretaceous detachment system (Richard et al. 1994, Siddoway et al. 2004a, Siddoway et al. 2005, Siddoway 2008, McFadden et al. 2010a, McFadden et al. 2010b, McFadden et al. 2015).

Magmatic arcs within greywacke-dominated accretionary orogenic settings are effective granite production factories (Vielzeuf et al. 1990, Brown 1994), particularly along advancing to transpression boundaries wherein crustal thickening occurs and deformation can enhance the physical and chemical segregation, migration, and coalescence of melts (e.g. Hollister & Crawford 1986, Brown 1994). Within the Fosdick Mountains, correlatives of the Ford Granodiorite suite and Swanson Formation were twice subjected to granulite facies conditions that produced voluminous anatectic granite from biotite-breakdown melting (Korhonen et al. 2011). The initial episode, broadly contemporaneous with Paleozoic arc magmatism, entailed conditions of $T = 820\text{--}870\text{ }^{\circ}\text{C}$, $P = 750\text{ to }1150\text{ MPa}$ (7.5–11.5 kbar) (Fig. 3-9a), as determined from mineral equilibrium modeling (Korhonen et al. 2010a, Korhonen et al. 2011). In paragneisses, a prevalent

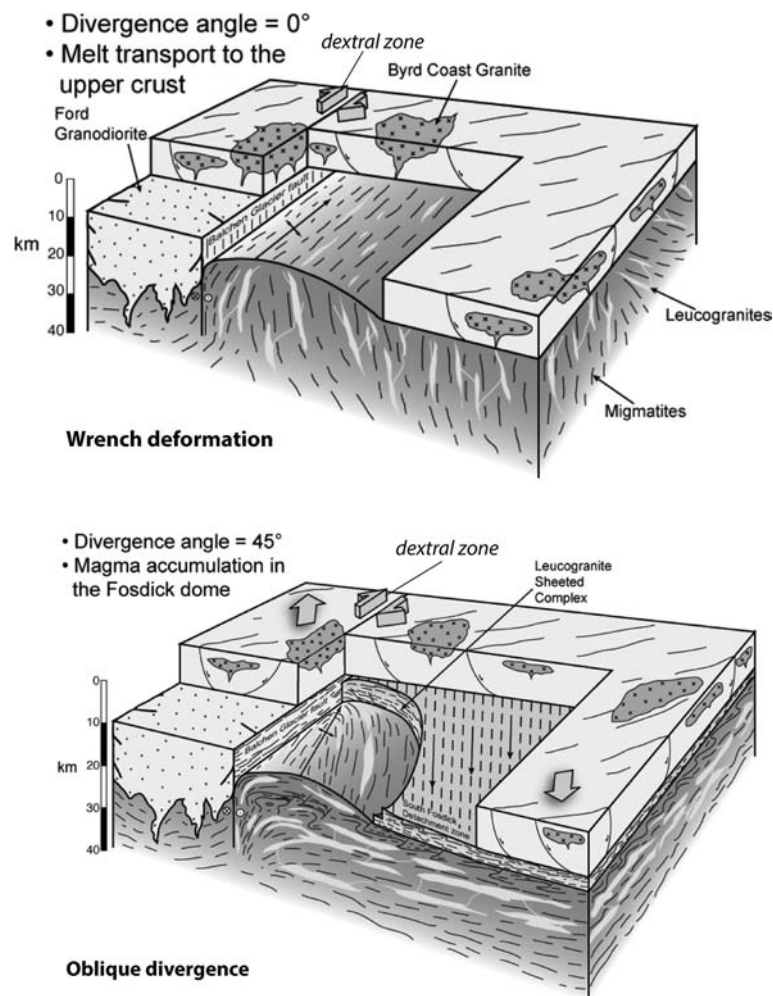


Fig. 3-11. Three-dimensional block diagrams that illustrate the structures developed during melt-present conditions in the middle crust in Marie Byrd Land during Cretaceous oblique convergence on the Gondwana margin (McFadden et al. 2010a). Exposures of migmatite and granite in the Fossdick Mountains gneiss dome reveal: a) an initial, strike-slip-dominated phase of deformation at 117 to 114 Ma, associated with steep fabrics and vertical pathways for melt migration, and b) a subsequent stage of oblique divergence from at 109 to 102 Ma, deformation and shows the Fossdick dome as a magma accumulation zone.

mineral assemblage is sillimanite-garnet-biotite \pm cordierite, associated with cordierite-bearing anatectic granites (Siddoway et al. 2004b). This widespread residual assemblage is not retrogressed, an indication of the extraction of anatectic melt and migration of melt and fluids out of the source region. Geochemical and isotope evidence from Ford Granodiorite suite and isotope evidence from zircon extracted from diverse plutonic phases in the Fossdick Mountains and Ford Ranges reflect the processes of crustal melting and differentiation that occurred in the Ross Province during middle Paleozoic orogenesis (Pankhurst et al. 1998, Korhonen et al. 2010a, Korhonen et al. 2010b, Yakymchuk et al. 2015).

The Cretaceous Gondwana margin (Fig. 3-6b) experienced oblique convergence between the Phoenix oceanic plate and Gondwana (Sutherland & Hollis 2001, Larter et al. 2002, Seton et al. 2012). Stretching axes oriented azimuth 074 – 254, oblique to the convergent boundary, are determined from orientations of fold axes, mineral stretching lineations, and the geometries of mafic and felsic dike arrays in the Ford Ranges and within the Fosdick Complex, corresponding to dextral transcurrent strain ~~on land in the Ford Ranges~~ (Siddoway et al. 2004b, Siddoway et al. 2005). High angle faults are delineated by steep geophysical gradients (Luyendyk et al. 2003) and contrasting mineral cooling ages between ranges (Richard et al. 1994, Siddoway et al. 2004b, McFadden et al. 2015).

Transcurrent deformation coincided with a second stage of granulite facies metamorphism and anatexis/biotite breakdown in the Fosdick migmatite-granite complex, with $T = 830\text{--}870\text{ }^{\circ}\text{C}$ and $P = 600\text{ to }750\text{ MPa}$ (6–7.5 kbar) (Korhonen et al. 2010a, Korhonen et al. 2011). The steep foliation imparted by early wrench deformation provided a pathway for granite migration to higher crustal levels at circa 117 to 114 Ma. Anatectic granites within vertical dikes that crystallized at 117 to 114 Ma (U-Pb zircon) underwent vertical shortening deformation. A change to oblique extension oriented $055^{\circ}\text{--}235^{\circ}$ led to the development of dilatant zones into which anatectic granites migrated. Thick subhorizontal sheets of cumulate granite were emplaced and crystallized from 109 to 101 Ma, coincident with onset of the normal-oblique South Fosdick detachment system. Stacked, sheeted granite intrusions immediately underlie the South Fosdick detachment zone (McFadden et al. 2010a, McFadden et al. 2010b). Within the ~2 km thick detachment zone (Fig. 3-11), solid state mylonitic fabrics are successively overprinted by kinematically compatible discrete brittle faults. Together the sequential structures provide a record of unroofing of the Fosdick dome (McFadden et al. 2010a, McFadden et al. 2010b); this is corroborated by mineral cooling ages (McFadden et al. 2015).

The past decade of research has produced U-Pb zircon geochronology and $^{40}\text{Ar}/^{39}\text{Ar}$ hornblende and biotite thermochronology at high spatial resolution for the Fosdick Mountains (McFadden et al. 2015, and references therein) and the Ford Ranges (Richard et al. 1994, Lisker & Olesch 1998, Contreras et al. 2012). In the Fosdick Mountains, U-Pb zircon crystallization ages of 102 Ma for youngest anatectic granites coincide spatially and temporally with $^{40}\text{Ar}/^{39}\text{Ar}$ cooling ages for hornblende (103 to 101 Ma) and biotite (101 to 100 Ma) in granitoids. The data indicate cooling rates $>100\text{ }^{\circ}\text{C}/\text{m.y.}$ that are a consequence of near-isothermal decompression and detachment-induced exhumation of hot, deep migmatites and granites to shallow crustal levels where conductive heat loss led to rapid cooling. A similar evolution of granite crystallization, exhumation, and rapid cooling is documented for Edward VII Peninsula (Fig. 3-1) at ca. 100 Ma (Siddoway et al. 2004a, Yakymchuk et al. 2015). Apatite fission track (Richard et al. 1994, Lisker & Olesch 1998) and (U-Th)/He zircon (Contreras et al. 2012) thermochronology research yields a dominance of ages between 96 to 87 Ma for samples from upper elevations, and scattered results down to 67 Ma from lower sites, reflecting a broad regional extent of Cretaceous tectonism in western Marie Byrd Land. The apparent absence of Cenozoic cooling ages likely is a consequence of tectonic stability and stabilization of lithosphere in western MBL since the time of breakup of MBL-Zealandia (Fig. 3-6b), an interpretation that is supported by the presence of thicker and faster lithosphere beneath this sector of West Antarctica (Heeszel et al. 2016).

Pleistocene alkali basalt lavas occur in small centers and as subvertical dikes across the Fosdick Mountains (Gaffney & Siddoway 2007). The lavas are of limited extent but high importance because they are mineralogically and chemically diverse and contain ultramafic xenoliths. The lavas have incompatible element enrichment patterns that

resemble those of the central and east Marie Byrd Land volcanoes (see below), but they have differing Sr-Nd-Pb isotope compositions. The xenoliths (Chatzaras et al. 2013, Chatzaras et al. 2016) represent a range of depths, and so may illuminate mantle conditions in zones of seismic anisotropy. The xenoliths display a great deal of variation in rock fabric, deformation intensity and mechanisms of deformation, as well as a wide range of equilibration temperatures of 780 to 1065 °C, based on pyroxene geothermometers and olivine-spinel Fe-Mg exchange geothermometry (calculated at $P = 1500$ MPa [15 kbar]). The wide range of temperatures of equilibration at approximately 50 km depth provides an indication of heterogeneities in the mantle beneath MBL, consistent with the variation in seismological characteristics that is being discovered for Marie Byrd Land (Accardo et al. 2014, Lloyd et al. 2015, Heeszel et al. 2016). The subcontinental lithospheric mantle of once-neighboring Zealandia is similarly heterogeneous (Scott et al. 2014).

3.4. Thurston Island/Eights Coast

Sparse rock exposures in the Thurston Island–Eights Coast terrane (Figs. 3-1, 3-3) yield a surprisingly detailed record of Late Carboniferous through Mesozoic calc-alkaline plutonism (Grunow et al. 1991, Storey et al. 1991, Leat et al. 1993, Pankhurst et al. 1993, Kipf et al. 2012, Riley et al. 2017b). Nd and Sr model ages indicate a maximum age of 1150–1400 Ma for underlying crust (Pankhurst et al. 1993), resembling the result from granitic orthogneiss of Haag Nunataks (Millar & Pankhurst 1987). The earliest U-Pb zircon isotopic age of circa 349 Ma for metaplutonic ‘basement’ rocks is very close in age to the Carboniferous granites of the Ross Province, suggesting a genetic association (Riley et al. 2017b). Subsequently, gabbro and diorites formed during Permian-Triassic mafic magmatism, at circa 239 Ma based upon U-Pb zircon geochronology (Riley et al. 2017b), potentially as a part of the broader convergent margin magmatism that is better recorded in the Antarctic Peninsula. Those rock formations had previously been constrained by $^{87}\text{Sr}/^{86}\text{Sr}$ determinations of 309 ± 5 Ma and mineral cooling ages of 240–220 Ma (Leat et al. 1993, Pankhurst et al. 1993). Jones Mountain granite, emplaced at circa 200 Ma, ties the region to more widespread magmatism that occurred in the Antarctic Peninsula and Ellsworth-Whitmore Mountains. The majority of Mesozoic I-type magmatism occurred in pulses, with one at ca. 182 Ma involving silicic volcanism, followed by activity at 157 to 145 Ma (Riley et al. 2017b) and 108–90 Ma. This Thurston Island evidence contributes to the evidence of the broad regional magmatism in middle Cretaceous time. Subduction of oceanic crust is indicated by initial $^{87}\text{Sr}/^{86}\text{Sr}$ ratios of 0.705–0.706 and Ndt values of +2 to –4, revealing the presence of juvenile lower crust or slightly enriched mantle along the Andean-type subduction margin of Gondwana. The Late Jurassic evolved magmas that dominate the record in Thurston Island resemble but are temporally distinct from the middle Jurassic granitoids in other sectors of the convergent margin such as the Antarctic Peninsula and Patagonia (Pankhurst et al. 1993).

A small contribution from crustal melts in Early Jurassic time is reflected by muscovite-bearing granite with an age of 198 ± 2 Ma, initial $^{87}\text{Sr}/^{86}\text{Sr}$ ratio of 0.710, and Ndt values of –5 to –7. Silicic volcanism from 100 to 90 Ma in the Jones Mountains produced lavas and tuffs that have $^{87}\text{Sr}/^{86}\text{Sr}$ initial ratios of 0.706–0.709 and Ndt values of –3 to –6 (Leat et al. 1993), suggesting crustal anatexis and a link to the intracontinental extension within the West Antarctica rift system (cf. Mukasa & Dalziel 2000, Yakymchuk et al. 2015) rather than to the long-standing subduction margin. Mafic dikes of Late Cretaceous age (ca. 90 Ma; Leat et al. 1993), oriented parallel to the coast of Thurston Island, cut the

older rocks. Granodiorite in the easternmost exposure of the terrane, at Lepley Nunatak, has an initial $^{87}\text{Sr}/^{86}\text{Sr}$ ratio of 0.7066 and a low ϵ_{Nd} value, suggestive of crustal contributions. New U-Pb zircon data provide an age of ca. 108 Ma (Riley et al. 2017b), with a constraint on cooling and thermal evolution provided by a $^{40}\text{Ar}/^{39}\text{Ar}$ biotite age of ca. 87 Ma (Pankhurst et al. 1993). The Jones Mountains also host pillowed alkalic basalts and palagonitized volcanoclastic rocks (Hole & LeMasurier 1994) of Miocene age (~10 Ma) that reach a thickness of 700 m. The primitive lavas have unradiogenic Sr-isotope ratios of 0.703, radiogenic Nd, and low large ion lithophile element concentrations, indicative of an aethenospheric source (Hole & LeMasurier 1994).

Contemporary tectonism at the margins of the Thurston Island terrane is indicated by Holocene volcanism in the Hudson Mountains (ca. 2 ka, Corr & Vaughan 2008), narrow subglacial rifts (Bingham et al. 2012), geophysical and heat flow anomalies (Jordan et al. 2010), and new thermochronology data that reveal differential cooling histories across physiographic lineaments (Lindow 2014, Spiegel et al. 2016). The exhumation of a gabbro intrusion from 3 km depth at ca 29 to 27 Ma (Rocchi et al. 2006) and apatite thermochronometry data indicative of rapid bedrock cooling at 29–25 Ma (Lindow 2014, Spiegel et al. 2016) are potential signs of fault reactivation or rift propagation along the boundary between the Thurston Island and Antarctic Peninsula terranes.

The Thurston Island and Eights Coast blocks are separated by and bounded on the west by tectonic basins. On the west, airborne gravity data (Cochran et al. 2015) reveal a well-defined sedimentary basin within the continental shelf of the Amundsen Sea Embayment. The basin accommodated 80–100 km of extension ($\epsilon = 1.5$ to 1.7) and contains a thickness of approximately 6 km of sediment. The basin margin abuts the dominant granitic rocks of the Thurston Island and Eights Coast blocks, and cuts across a system of east-west trending, stepped half-grabens that separate the two blocks. The grabens correspond to an elongate depression formed by distributed, minor extension, that now is occupied by seawater supporting the Abbott Ice Shelf (Bingham et al. 2012). The grabens' orientation parallel to the Cretaceous mafic dyke array on Thurston Island (Leat et al. 1993), and their gravity characteristics, suggest that they formed during the onset of rifting between West Antarctica and Zealandia (Cochran et al. 2015). Breakup ultimately localized along the north margin of Thurston Island and eastern Marie Byrd Land.

3.5. West Antarctic Rift Province

Covering an area of $\sim 1.2 \times 10^6 \text{ km}^2$, the vast West Antarctic rift system (WARS) is comparable to other active rift provinces on Earth from the standpoint of aerial extent and range of geotectonic characteristics (LeMasurier 2008). The system's interior margin exhibits some of the most dramatic topographic relief found on Earth's continents (Fig. 3-1), with a vertical exchange of 7700 meters between the deepest subglacial low and highest neighboring summits. Within the WARS there are profound, narrow deeps, including the Bentley subglacial trench and Byrd Subglacial Basin, that likely are structurally controlled (Winberry & Anandakrishnan 2004, Jordan et al. 2010, Chaput et al. 2014). The deep troughs have been attributed to Oligocene transcurrent faults reactivated under extension (Granot et al. 2013) or grabens formed during Cretaceous extension (Trey et al. 1999). The Bentley subglacial trench coincides with the north boundary of the Ellsworth-Whitmore Mountains terrane (Lloyd et al. 2015).

The region of the WARS is characterized by thin crust, high heat flow, active volcanism, and presence of low velocity, low viscosity, warm mantle (Behrendt et al. 1991a,

Behrendt et al. 1994, Behrendt et al. 1996, Behrendt 1999, Ritzwoller et al. 2001, Danesi & Morelli 2001, Pollard et al. 2005). It hosts active seismicity of moderate magnitude: in 2012, there were four tectonic earthquakes of M.4.4 to M5.5 in the southern Ford Ranges of Marie Byrd Land (USGS Earthquake Hazards Program, accessed May 2015) – some of the first to be recorded within the continental crust of West Antarctica (cf. Reading 2006). Elevated heat flow of 83 to 126 mW/m² occurs across the WARS (Blackman et al. 1987, Berg et al. 1989), with flux as high as 285±80 mW/m² at one locality (Fisher et al. 2015). The WARS is the only active continental rift province on earth to host a polar ice sheet during a time of rapid glaciological change, making it a feature of considerable contemporary scientific interest.

West Antarctica's subglacial topography now is known with improved resolution, since the release of BEDMAP2 gridded surface elevation, ice-thickness, bathymetry and subglacial bed elevation data (Fretwell et al. 2013). Surface topography is becoming available for the first time as a result of new methods of digital elevation model (DEM) extraction from high-resolution stereoscopic Worldview 1 & 2 imagery (e.g. Porter et al. 2011, Noh & Howat 2015). Advances in characterization of the geophysical properties of the lower lithosphere and asthenospheric mantle are being achieved via the A-NET and POLENET GPS and seismic networks upon Antarctica (<http://polenet.org>).

The international research efforts that are bringing West Antarctica into focus provide a foundation for contemporary research in West Antarctica, banishing long-standing enigmas that exist for the dominantly ice covered region. These include: the character of West Antarctica crust and lithosphere (e.g. Behrendt et al. 1996, Bell et al. 1998, Luyendyk et al. 2003, Handler et al. 2003, Chaput et al. 2014); the tectonic context for Neogene to present alkaline magmatism (Finn et al. 2005, Rocchi et al. 2006, Sutherland et al. 2010); the causes for Cenozoic tectonic reactivation (e.g. Rossetti et al. 2003b, Salvini et al. 1997, Paulsen & Wilson 2010) and seismicity (Winberry & Anandakrishnan 2004, Lough et al. 2013), and the influence of inherited structures upon ice-ocean-bedrock interactions of the dynamic West Antarctic ice sheet (Lowe & Anderson 2002, Vaughan et al. 2006, Holt et al. 2006, Sorlien et al. 2007, Gohl 2011) during contemporary climate change (Jordan et al. 2010, Bingham et al. 2012).

Knowledge of the Mesozoic tectonic evolution of the WARS within Gondwana also is critical to understanding of geological complexity and regional variations arise from structural inheritance (e.g. Lowe & Anderson 2002, Siddoway 2008, Vaughan et al. 2006, Holt et al. 2006, Sorlien et al. 2007, McFadden et al. 2010b) and the Cretaceous to present landscape evolution (LeMasurier & Landis 1996, LeMasurier 2006, Bialas et al. 2007, Huerta 2007, Wilson & Luyendyk 2006, Wilson et al. 2012). Mesozoic structures reactivated within the late Miocene to present tectonic framework commonly coincide with sites of dynamic ice-bedrock interactions for the West Antarctic ice sheet (Paulsen & Wilson 2009, Granot et al. 2010, Granot et al. 2013, Gohl 2011, Kipf et al. 2014).

3.5.1. Character of crust and lithosphere

Crustal thickness <28 km for the rift province (Figs. 3-2, 3-12) is determined from seismic refraction, seismic reflection, and gravity data (Trey et al. 1999, Luyendyk et al. 2003, Wobbe et al. 2012), broadband seismic data (Winberry & Anandakrishnan 2004), gridded effective topography (Müller et al. 2007; see also references therein) and seismic receiver functions of P- to S-wave conversions (Chaput et al. 2014). These differing and complementary methods all determine 21 to 28 km thicknesses for the broad arcuate

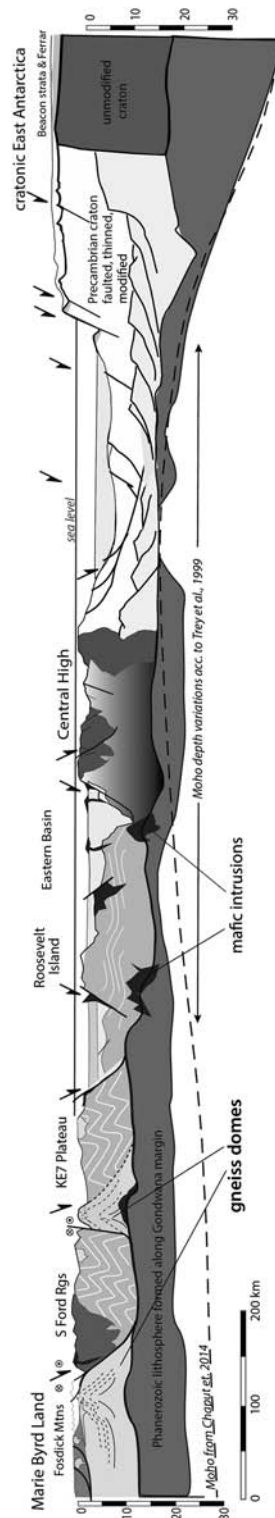


Fig. 3-12. Schematic profile across Marie Byrd Land and the Ross Embayment (Tinto et al. 2018), view toward South, with Marie Byrd Land on left and Transantarctic Mountains part sector of East Antarctica on right. Vertical exaggeration: 5x. Grey colors on left denote distal, marine, deeper water sediments derived from Ross Orogen, and underlying lithosphere. White and pale grey colors denote terrigenous to shallow marine, proximal sediments derived from Ross Orogen, and underlying basement of 600 to 170 Ma age, upon faulted lithosphere. Other crustal elements are as labeled on diagram. Two contrasting Moho profiles are provided: black line, seismic discontinuity and velocity contrast of Trey et al. (1999); pink line, P- to S-wave conversion of Chaput et al. (2014).

region that extends from the Ross Sea and Ice Shelf to the Thurston Island block, with somewhat thicker crust, up to 32 km thick (Luyendyk et al. 2003, Chaput et al. 2014), underlying the region of highest topography in central Marie Byrd Land.

Continental crust of the continent–ocean transition zone (Fig. 3-13) north of Marie Byrd Land, that has only sparse volcanism, is 24 km thick, based on new marine gravity and seismic reflection data (Wobbe et al. 2012). Bordering the Ross Sea and western Marie Byrd Land, the margin is steep and abrupt (Lawver & Gahagan 1994, Cooper et al. 1991b), and the width of the zone is 145 km, quite narrow when compared to the 670 km wide transition zone in the Bellingshausen Sea, where there is abundant magmatism. The age of the first definitive oceanic crust is 84 Ma, based on the identification of magnetic anomaly c34y (McAdoo & Laxon 1997, Wobbe et al. 2012). Magnetic anomalies mapped in the Amundsen Sea embayment, that are interpreted on the basis of gravity characteristics to be mafic intrusions, are attributed to continental rifting-related magmatism between 100–85 Ma, preceding breakup between Zealandia and Marie Byrd Land.

Extension factors are $\beta = 1.3$ to 1.8 based on Müller et al. (2007) crustal thinning grid derived from effective topography (sedimentary cover, removed) relationships. Thin crust (~25 km) along the south flank of Marie Byrd Land corresponds to high topography, with bedrock elevation 1000 m greater than is predicted by Airy isostasy (Winberry & Anandakrishnan 2004, cf. LeMasurier & Landis 1996). The lack of isostatic compensation corroborates the evidence from seismic velocity anomalies for low-density mantle beneath southern MBL that contrasts with average-density mantle beneath the interior of the rift (Winberry & Anandakrishnan 2004).

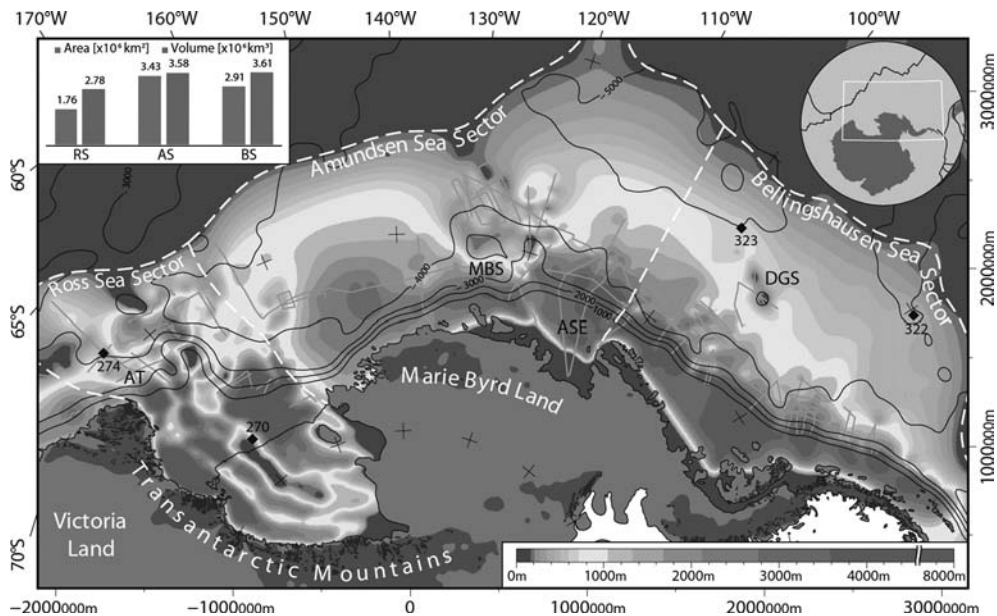


Fig. 3-13. Map of sediment thicknesses within marine shelf/basins bordering West Antarctica, from Wobbe et al. (2014). Contours correspond to water depth, in meters, and isopach thicknesses are according to the barscale. Sediment catchment areas are delineated by dashed lines; coverage area and estimates of compacted sediment volume are given by histogram in upper left. DSDP sites are annotated with black diamond symbol. Abbreviations: RS = Ross Sea, AS = Amundsen Sea, BS = Bellingshausen Sea, AT = Adare Trough, DGS = De Gerlache Seamounts, MBS = Marie Byrd Seamounts.

The most profound depths and thinnest crust correspond to the Byrd Subglacial Basin, Pine Island Rift and Ferrigno Rift (Figs. 3-1, 3-2), where the depth to Moho is determined to be 19 ± 1 km (Jordan et al. 2010, Bingham et al. 2012, Chaput et al. 2014). The narrow dimension and linearity of the features are suggestive of steep structural geometries associated with transform faults, an interpretation that is supported by kinematic models derived from Cenozoic plate circuits (Müller et al. 2007, Granot et al. 2013). The deep trenches and troughs therefore may have originated as releasing bends (Müller et al. 2007), or occupy strike slip faults that have been reactivated by extensional deformation (Jordan et al. 2010, Bingham et al. 2012).

3.5.2. Bedrock structures' influence upon ice-ocean dynamics

A focus of much contemporary research is the deep, narrow bathymetric features that underlie the West Antarctic ice streams in eastern Marie Byrd Land and Thurston Island, because they coincide with sites of dynamic thinning of the West Antarctic ice sheet (Jordan et al. 2010, Bingham et al. 2012). The narrow channels allow infiltration/circulation of warm ocean water beneath the ice sheets. A zone of elevated geothermal heat flow is known to underlie one of these narrow rift areas so far (Schroeder et al. 2014). Thermal anomalies are likely to correspond with reactivated faults within subglacial bedrock and sites of Pleistocene-Holocene active volcanism (Wilch et al. 1999, Gaffney & Siddoway 2007, Corr & Vaughan 2008, Narcisi et al. 2006, Lough et al. 2013). The question of basal geothermal flux arising from warm mantle beneath thinned crust (Maule et al. 2005, Shapiro & Ritzwoller 2004, Lawrence et al. 2006a, Lawrence et al. 2006b) is of obvious consequence for ice sheet dynamics. There is pressing need to determine the influence of underlying crustal structures on heat flow, volcanism, basal melting, and influx of marine waters, that have immediate effect on the stability of glaciological and glacial-marine systems that are subject to atmospheric and ocean warming (e.g. Jordan et al. 2010, Bingham et al. 2012, Feldman & Levermann 2015).

3.6. Tectonic Evolution and Timing of the WARS

3.6.1. Relationship between the Transantarctic Mountains and West Antarctic rift system

The spatial correspondence of the WARS' western and southern limits of thinned crust with the dramatic mountain relief of the Transantarctic Mountains (Figs. 3-1, 3-12) has naturally led to investigation the following questions: 1) did the high topography and curvilinear front of the Transantarctic range originate at the same time and within the same tectonic framework as broad extension across the WARS, during narrow extension in the Terror Rift, or a combination of both? and 2) How thick and how high was the crust of West Antarctic prior to extension?

There is ongoing debate and an array of different standpoints on these two questions. The first question has been investigated through apatite fission track thermochronology and multi-method thermochronometry (e.g. Glorie et al. 2012), and geodynamics, and the second has been explored via kinematic and thermal-mechanical models and paleotopographic reconstructions that track eroded sediment volumes. The sparse on-land sedimentary deposits and small number of deep drill cores prevent the use of traditional

stratigraphic methods that would allow reconstruction of the uplift and exhumation history (e.g. Lisker & Läufer 2013). Thermochronology data (multiple $^{40}\text{Ar}/^{39}\text{Ar}$ mineral systems, and low temperature thermochronology data from zircon (U-Th)/He, apatite fission track, and apatite (U-Th-Sm)/He systems), therefore, provide the current basis of understanding of the stages of landscape evolution of the TAM-WARS.

Apatite fission track **ages** for the TAM have been interpreted in terms of both differential or possibly episodic denudation between crustal blocks separated by crustal-scale structures, in the Cretaceous to Paleogene (Fitzgerald 1994, Fitzgerald 2002, and references therein), *or* as a record of subdued topography and sedimentary burial throughout the Mesozoic, followed by Cenozoic extension (Lisker & Läufer 2013).

Cretaceous episodes of cooling are recorded in south Victoria Land (Fitzgerald 2002, and references therein), north of David Glacier (Balestrieri et al. 1997), and across a transect of the Pacific margin of north Victoria Land (Lisker 2002), overlapping in time with the formation of the Ross Sea epicratonic basins (Figs. 3-12, 3-14). Three to 4 km of sediments accumulated in the generally north-south-oriented elongate **basins**, **mafic** magmatism occurred, corresponding to regions of high seismic velocities and gravity anomalies at 6 to 11 km in the upper crust (Trey et al. 1999). Regional denudation of 2 to 3 km is interpreted for the Mesozoic, with a modest volume of eroded detritus provided to Ross Sea basins and depocenters at the continent-ocean boundary (Karner et al. 2005, Decesari et al. 2007, Wilson et al. 2012). A fairly wide range of **ages** span the broad extension phase in the WARS, and overlap with the time of breakup between Australia-East Antarctica and West Antarctica-Zealandia. Correspondingly, there must have been

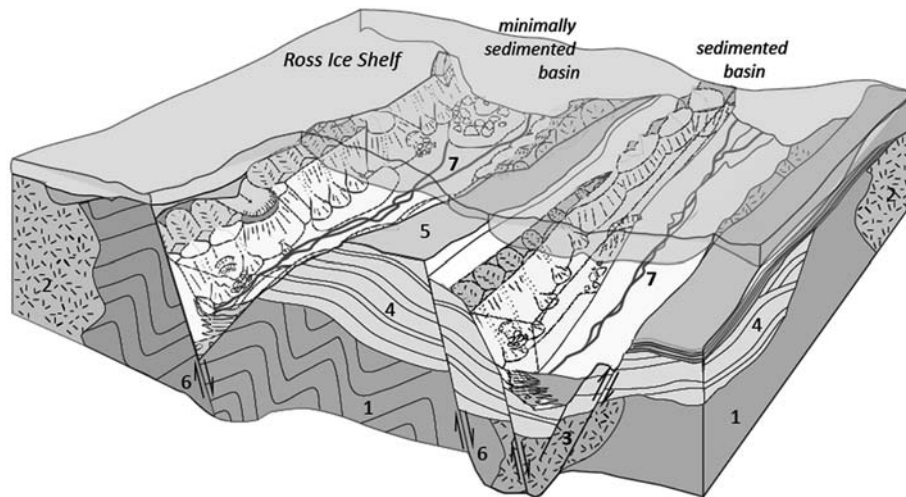


Fig. 3-14. (a) Map of sedimentary basins (shaded grey) of the Ross Sea, from Decesari et al. (2007). Basins are delimited by a depth to basement greater than 2.5 km (ANTOSTRAT 1995). Abbreviations are VLB: Victoria Land Basin, NB: Northern Basin, CT: Central Trough, and EB: Eastern Basin. The location of Deep Sea Drilling Program sites 270 and 272 are indicated with numerals. The bold line denotes the location of seismic profiles collected orthogonal to the basin structure (ANTOSTRAT 1995, Trey et al. 1999, Buseti et al. 1999). (b) Bathymetric profile with geo-tectonic interpretation of a modelled profile that closely parallels the seismic transect indicated with a bold line in (a), from Buseti et al. (1999). The tectonic basins contain Late Cretaceous (?) early rift sediments through Palaeogene basin fill/The basin deposits and intervening basement highs are overlain unconformably by Neogene glacial and glacio-marine sediments. The Moho, designated with a solid line, is interpreted on the basis of refraction and OBS data, and 2-D gravity models.

a development of mountain relief in the TAM at circa 115 to 100 Ma, in agreement with a new geodynamic model and plate tectonic reconstruction of East Gondwana by Jacob & Dymant (2014). Using first order conjugate features and pseudo-isochron/gravity anomalies between Australia, East Antarctica and West Antarctica, Jacob & Dymant's (2014) reconstruction predicts lithospheric thickening and the development of topographic relief in a linear belt corresponding to the TAM. If correct, the reconstruction provides a plausible framework for the development of an orogenic plateau that has been proposed by some (Bialas et al. 2007, Huerta & Harry 2007).

Apatite fission track data indicate a rapid cooling interval in the Eocene Epoch, also, attributed to rapid bedrock uplift at rates of 100 to 200 meters per million years (Sugden et al. 1995, Busetti et al. 1999, Fitzgerald 2002) and denudation on the order of 4 to 10 km. Tectonism related in part to seafloor spreading in the Adare Trough, where there was 160 km of spreading between 40 and 26 Ma (Granot et al. 2013). The focused extension in the Adare Trough within the Antarctic Plate was accompanied by distributed extension in the Ross Sea basins (Karner et al. 2005), with 95 km of extension in the Victoria Land Basin (Davey et al. 2006) and stretching of 40 km in both the Central and Eastern Basins (Decesari et al. 2007). Supporting evidence for this comes from thermal subsidence models of the eastern Ross Sea's broad marine platforms, regionally extensive surfaces that have been depressed to depths of 100 m to 350 m below sea level (Wilson & Luyendyk 2006). Investigators of the landscape evolution on the margins of the RIS (Lisker & Läufer 2013, Foley et al. 2013) have recently challenged the established view that the topographic relief between TAM and the West Antarctic rift province is a product of episodic uplift since 55 Ma, however.

A final phase of tectonism that is recorded by thermochronology and basin sedimentation is Oligocene-Miocene, from 34–23 Ma. The period is marked by formation of prominent incised troughs separated by bedrock highs, interpreted as a product of intense localized erosion after onset of continental glaciation at ca. 34 Ma (e.g. Sorlien et al. 2007, Lisker & Läufer 2013) or even later, at ca. 14 Ma when there was a shift toward warm-based glaciation (e.g. Stern et al. 2005, Sugden et al. 2005). Seismic stratigraphic records for the Ross Sea provide information about the volume of sedimentary detritus transferred from 'continental' Marie Byrd Land to depocenters in the Ross Sea and on the continental shelf (e.g. Wilson et al. 2012, Wobbe et al. 2012). The least-known Central and Eastern basins contain records that reflect large scale regional systems, whereas the Victoria Land and Northern basins contain sediments derived from proximal sources in the Transantarctic Mountains (De Santis et al. 1999, Wobbe et al. 2012).

Although there is a lack of consensus about the time of formation, origins of the dramatic relief of the Transantarctic Mountains, and relationship to the West Antarctic rift system, there nevertheless is an impetus to obtain a resolution to the issue due to the need for tighter constraints on the timing and kinematics of relative motions within West Antarctica for development of a robust tectonic plate circuit for the southwest Pacific (Matthews et al. 2015, Granot et al. 2013, and references therein). A synthesis here follows of the geological and geochronological factors that bear on the extent and timing of the West Antarctic rift system.

3.6.2. Mesozoic development

The origins of the West Antarctic rift system (WARS) date to the time of Pangaea breakup and Jurassic crustal extension between East and West Gondwana. The emplacement of Ferrar Dolerite (Fleming et al. 1997, Elliot & Fleming 2004, Fleming 2008, Leat

2008) and opening of the Weddell Sea (Grunow et al. 1987, Jokat et al. 2003, Veevers 2012) mark this initial stage that formed an early part of what became the WARS. The Ferrar tholeiitic sills and associated volcanic rocks span a phenomenal 3500 km length of the margin of East Antarctica, yet were emplaced in a span of just 1 million years at circa 183 Ma (Fleming et al. 1997, Elliot & Fleming 2004, Leat 2008). The Weddell Sea opened in two stages, as evidenced by marine magnetic anomalies identified from marine geophysical surveys (König & Jokat 2006, Jokat 2007) and potential fields data (Jordan et al. 2013). The first deep continental rift basin to develop at circa 167 Ma Ma was the Somali-Mozambique basin between Queen Maud Land, India-Sri Lanka, and southern Africa (Mozambique). The connection from Africa (Natal Embayment) was unbroken (Fig. 3-3). At ca. 147 Ma, slow separation between the Antarctic Peninsula, southern South America and Africa commenced, with creation of true ocean floor in the western Weddell Sea. Restricted sedimentation began, but communication between the Weddell Sea and Somali-Mozambique basins was not yet established.

During the Cretaceous, a dramatic episode of intracontinental extension affected central West Antarctica and Zealandia, that at the time were contiguous within East Gondwana. The term *Zealandia* refers to the entirety of the continental landmass of New Zealand, including the submerged portions of the Campbell Plateau, Lord Howe and Chatham Rises (Fig. 3-6b). In less than 20 million years, central West Antarctica underwent 600 kilometres of extension, and across the Ross Sea through western Marie Byrd Land, >1000 kilometres of stretching occurred (DiVenere et al. 1996, Luyendyk et al. 1996, Storey et al. 1999). The broad basin beneath the Ross Sea and Ice Shelf formed, and the Bentley/Byrd troughs (Fig. 3-1) were created (Cooper et al. 1991b, Lawver & Gahagan 1994, Davey & Brancolini 1995). In New Zealand, the Campbell Plateau/Great South Basin developed (Fig. 3-6b) (Sutherland 1999, Grobys et al. 2009). Plate separation between West Antarctic and Zealandia occurred along a trend orthogonal to the rift basins (Siddoway 2008; see Fig. 3-6b). Tectonic restoration of the abrupt, steep, rifted margins of the two land masses produces a tight fit of the already-extended crust, providing clear evidence that major extension across West Antarctica occurred prior to breakup at 83 Ma (Lawver & Gahagan 1994, McAdoo & Laxon 1997). The degree of extension and timing of events in Antarctica are corroborated by structural/thermochronological data from extensional detachment faults at three sites spaced across 1000 km from the central Ross Sea to its eastern margin (Fig. 3-12) (Fitzgerald & Baldwin 1997, Siddoway et al. 2004a, McFadden et al. 2010b). Middle to lower middle crustal rocks were tectonically exhumed and cooled extremely rapidly between 110 to 96 Ma, well in advance of onset of seafloor spreading at 84–83 Ma (McAdoo & Laxon 1997, Eagles et al. 2004).

The ca. 100 Ma crustal thinning across MBL and the eastern Ross Sea-Ross Ice Shelf occurred within the context of distributed transtension, according to records from well-studied bedrock exposures within extended crust on the eastern margin of the Ross Sea (Siddoway et al. 2004b, McFadden et al. 2010a). The wrench component of deformation arose from the rapid oblique subduction of young, hydrated oceanic lithosphere of the Phoenix plate (Sutherland & Hollis 2001, Finn et al. 2005). Widespread rapid cooling (Siddoway 2008) led to landscape stabilization and formation of regionally extensive erosion surfaces at two or more elevations (LeMasurier & Landis 1996, Wilson & Luyendyk 2006). The lower, better-characterized erosion surface formed as a wavecut marine platform, based on the areal extent of the low relief surface that is unaffected by variations in rock type (Wilson & Luyendyk 2006). The erosion surface(s) provide a valuable datum for subsequent differential movements due to deformation, erosion,

isostatic adjustment in response to glacial loading/unloading, and/or thermal subsidence. There is indirect evidence for significant Eocene-Oligocene extension in the southern and eastern Ross Embayment (e.g. Cande et al. 2000, Granot et al. 2013), where there is evidence of broad thermal subsidence that cannot be accounted for by the lithospheric response to ice sheet loading/unloading, and must be post-middle Eocene (Wilson & Luyendyk 2006).

Beneath the Ross Sea, normal-fault-bounded basement highs and basins have been mapped from marine multichannel seismic surveys, ocean bottom seismograph, and gravity surveys (Cooper & Davey 1985, Cooper et al. 1987, Cooper et al. 1991a, Davey & Brancolini 1995, Trey et al. 1999). Interpreted as early-rift structures, the elongate, north-south-oriented basins display positive gravity anomalies and high seismic velocities in the lower crust, suggesting the presence of dense mafic igneous rock. Crustal thicknesses beneath the basins may be as low as 14 km, increasing to 21 to 24 km beneath the Coulman and Central Highs (Trey et al. 1999, Buseti et al. 1999, Chaput et al. 2014). The basement highs divide the Ross Sea sector of the rift into four basins: the Northern Basin, Victoria Land Basin, Central Trough, and Eastern Basin (Cooper et al. 1995). Prevalent normal faults bound the basins (Cooper et al. 1991a, Cooper et al. 1991b, Tessensohn & Wörner 1991), and tectonic lineaments marking transfer systems both partition the basins and segment the Transantarctic Mountains into blocks with differing levels of crustal exposure (Rossetti et al. 2003b). The basins contain a fill of 1 km to 4 km of inferred Mesozoic sedimentary fill, overlain by thin Paleogene deposits, and a thick accumulation of glacial sediments that expands beyond the bounds of the structural basins (Anderson et al. 2001, Karner et al. 2005). Bounded by faults that accommodated 6 km or more of relative motion (Hamilton et al. 2001), the Victoria Land Basin in the western Ross Sea contains a thickness of sediments up to 14 km (Cooper et al. 1987, Brancolini et al. 1995, Buseti et al. 1999).

For the region of the Ross Ice Shelf, where bathymetric and geophysical data coverage is sparse, it is nevertheless clear that accumulated sediments are thin or absent. BEDMAP2 bathymetry is dominated by elongate, narrow bedrock highs (Fretwell et al. 2013). There is no sediment upon the bedrock highs and only thin (200–600 m) sediments are found in the glacial troughs (Fig. 3-15) (Chaput et al. 2014, their Table 1). Gravity characteristics also differ from those of the Ross Sea region, in that the anomalies associated with the elongate bedrock highs indicate the presence of multiple types of bedrock, including both basement and sedimentary deposits (Wilson & Luyendyk 2006). An inherited structure, the Byrd Glacier fault zone, that has ~1 km of south-side-up relative motion since 40 Ma (Foley et al. 2013), appears to form the boundary between the Ross Sea and Ice Shelf regions.

In summary, considered in light of the temporal/denudational history of major topographic/bathymetric features, thermochronological data indicate that the present configuration of the WARS resulted from Mesozoic broad extension followed by Cenozoic narrow extension focused in the western Ross Sea. Diverse modeling approaches have been employed using elastic, kinematic and thermal-mechanical methods, to explore the two-stage extension. These include Stern & ten Brink (1989), Fitzgerald et al. (1986), Lawrence et al. (2006b), Bialas et al. (2007), Huerta & Harry (2007), and van Wijk et al. (2008).

Models for the West Antarctic rift system that emphasize the role of lithospheric-scale faults bounding the TAM include the crustal detachment model of Fitzgerald et al. (1986) and the flexural origin models of Stern & ten Brink (1989) and ten Brink et al. (1997). The moderately dipping crustal detachment acts as a transfer or relay linking

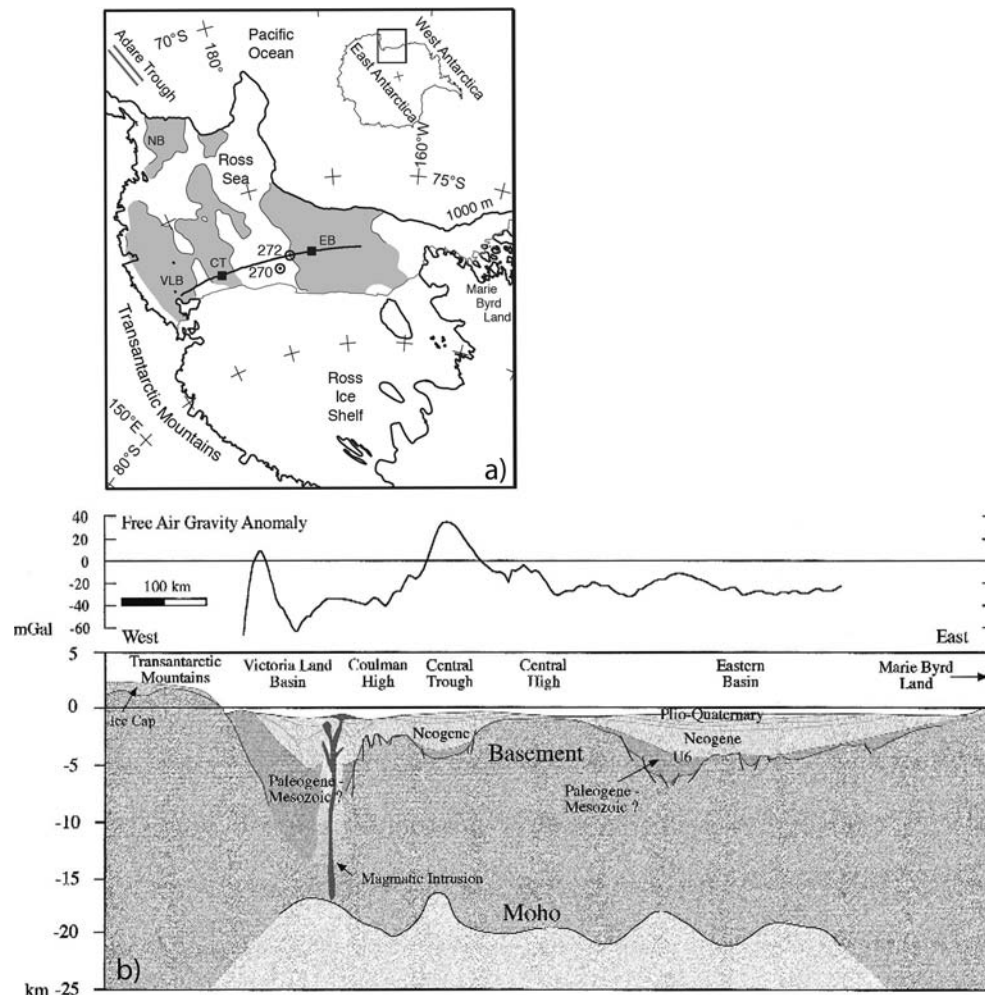


Fig. 3-15. Interpretive block diagram with schematic representation of bedrock units and bathymetric features beneath the Ross Ice Shelf, a region that appears to lack glaciofluvial sediments that elsewhere obscure the bedrock structure (e.g. Ross Sea). View is to southeast. Labels are: 1) Thick package of immature sedimentary rocks, low-grade metamorphosed (metagreywacke), intruded by 2) intermediate to felsic plutons (e.g. Yakymchuk et al. 2013). 3) Mafic igneous rocks, related to WARS development (e.g. Davey & Brancolini 1995). 4) Tertiary strata deposited after breakup between West Antarctica and New Zealand (e.g. Wilson et al. 2012). 5) Low relief surfaces at 100 to 350 meters below sea level, interpreted as remnants of a pre-glacial extensive wavecut platform (Wilson & Luyendyk 2006). 6) Inferred high angle normal faults of Mesozoic-Cenozoic origin (Davey & Brancolini 1995, Luyendyk et al. 2001). 7) Linear troughs formed by localized intense glacial erosion (e.g. Stern et al. 2005, Sorlien et al. 2007), ca. 700 mbsl, with moderate to small sediment thickness (cf. Chaput et al. 2014) suggestive of effective removal of detritus or young age of incision (mid-Miocene or younger).

the region of extensional strain in the upper crust, beneath the WARS, to the realm of subcrustal lithosphere extensional strain beneath the TAM (Fitzgerald et al. 1986). The lithospheric flexure models, by contrast, envision a steep normal fault separating extended West Antarctica from intact East Antarctica lithosphere, causing flexural uplift of the TAM due to lateral variations in temperature, density, and amount of erosion. Ten Brink

et al. (1997) assign the change in the effective elastic thickness across the TAM bounding fault to the Eocene. A role for anomalously warm asthenosphere created by rifting, crustal thinning and magma injections into the middle and lower crust of the rift zone, is a component of the thermally driven uplift models of Smith & Drewry (1984) and Berg et al. (1989). Recent work by Lawrence et al. (2006b) calls upon the dual effects of a buoyant thermal load and flexural uplift, at the juncture between warm, thin lithosphere underlying the WARS and the cold lithosphere of East Antarctica.

Other numerical models of viscoelastic-plastic, non-Newtonian behavior explore the consequences of extension across a speculative thick crust of an orogenic plateau formed during Mesozoic plate convergence and subjected to a range of thermal conditions (Bialas et al. 2007, Huerta & Harry 2007). In addition to the abrupt, faulted margin at the TAM, geological evidence of a “West Antarctic plateau” comes from the sedimentary detritus in the Triassic Beacon Supergroup in the Transantarctic Mountains, that is attributed to East Gondwana margin sources (Elliot & Fanning 2008), in particular, detrital zircon, interpreted to have been transported from the Mesozoic marginal arc across a forearc basin to the site of deposition in the TAM, or alternatively transported subaerially across a broad highland (e.g. Collinson et al. 1994). Another source of indirect evidence for elevated terrain in West Antarctica, albeit in Paleocene-Eocene time, is the thermal subsidence history of the extensive submerged bedrock platforms in the southern and eastern Ross Embayment (Wilson & Luyendyk 2006).

Still under consideration and debate, the numerical models for the formation of the TAM in the context of the WARS encompass mechanically driven uplift, thermal support, extensional collapse of a West Antarctic plateau, and combination models. Ongoing evaluation and refinement will need to take into account geological factors from rock records and refined knowledge of the character of lithosphere and mantle of West Antarctica.

3.6.3. The Cenozoic: tectonic sedimentation, structural reactivation, and seismicity

Intracontinental basin sediments

The record of the distribution and thickness of Cretaceous through Cenozoic sediments and sedimentary rocks in interior West Antarctica has been obtained principally through marine geophysical surveys in the Ross Sea and airborne geophysical surveys over interior West Antarctica and the Ford Ranges. Surveys of the past quarter-century are reported by Behrendt (1999), Behrendt et al. (1991a, 1991b), Cooper et al. (1995), Davey & Brancolini (1995), De Santis et al. (1995, 1999), Bell et al. (1998, 2006), Buseti et al. (1999), Luyendyk et al. (2001, 2003), Hamilton et al. (2001), Wilson & Luyendyk (2006), Sorlien et al. (2007), Fielding et al. (2008), and by works cited within those reports.

Young glacial and glacial marine sediments fill and conceal the fault-bounded bedrock highs and structural basins of the Ross Sea. The deposits form ridges of unconsolidated glacial detritus that extend seaward into sedimentary wedges with seaward dipping reflectors (Anderson et al. 2001). In between are elongate troughs. Exquisite mega-scale glacial lineations, drumlins, and gullies record the seaward transport of voluminous sediments and dynamic modifications by glacial meltwater.

Drilling recovery of sediment cores has been achieved at a few locations in the Ross Sea, by the Deep Sea Drilling Program (e.g. Hayes et al. 1975), Cape Roberts Project (Bohaty et al. 2000, Naish et al. 2001), CIROS (Barrett 1989) and ANDRILL projects (Antarctic Drilling Program 2015). Sampling of unconsolidated subglacial sediments has been achieved through use of hot water drilling to reach the base of the central West Antarctica ice streams and ice sheet (e.g. Tulaczyk et al. 1998, Licht et al. 2014).

The major Ross Sea basins are the Victoria Land Basin in the west, Central Trough, Northern Basin, and Eastern Basin (Figs. 3-12, 3-14). The Victoria Land Basin contains wedges of coarse-grained sediments deposited in fans and deltas within half-grabens, and in grabens deposited during an early rift phase (Fielding et al. 2008). These are bounded or truncated by active faults. The coarse sediment wedges are overlain by symmetrical, inward thickening lenses of cyclic shallow marine to glaciomarine sediments. Material of this type was sampled from Deep Sea Drilling Program Site 270, Leg 28, cored to 412 meters. The site was situated on the margin of a basement high, where drilling penetrated through the sedimentary deposits into 30 meters of regolith/sedimentary breccia, then an underlying carbonaceous metasedimentary complex (Ford & Barrett 1975, Mortimer et al. 2011). The regolith/breccia was formed subaerially, and it is overlain by thin (<5 m) margin-facies clastic rocks, specifically, carbonaceous quartz sand followed by glauconitic greensand. K/Ar dating of the glauconite yielded an age of circa 26 Ma. Above the sandstones are glaciomarine sediments of late Oligocene-early Miocene age, including >300 m of silty claystones with suspended granules and pebbles, capped by an angular unconformity. Plio-Pleistocene sediments above the unconformity are feldspathic sandstones containing granules (Ford & Barrett 1975).

Sites 271, 272, and 273 of the Deep Sea Drilling Program (DSDP) Leg 28 drilled in to sediments of the Central and Northern Basins of the Ross Sea (Hayes et al. 1975). Sites 271, 272, and 273 were cored to sub-bottom depths of 265, 443 and 346 meters, respectively. There was poor to no recovery of strata from the sites, and none contain pre-Miocene rocks. All four sites are dominated by lithified, unstratified, silty mudstone containing marine microfossils and sparse lithic clasts; the mudstones are of predominantly Miocene age. The cores provide 'ground truth' for the seismic stratigraphic units mapped across the Ross Sea (Brancolini et al. 1995, De Santis et al. 1995, Luyendyk et al. 2001, Sorlien et al. 2007), named the Ross Sea seismic (RSS) sequence and Victoria Land Basin seismic (V) sequence (Cooper et al. 1987). The RSS contains eight units separated by unconformities. The deepest sedimentary package is identified as syntectonic extensional deposits marked by inclined seismic reflectors that correspond to rotated bedding. The package is cut by faults, as evidenced by discontinuity of layers and tectonic breccia that was penetrated by the drill core recovery at DSDP site 270 (Ford & Barrett 1975, Ford 1991). The eastern Ross Sea basin displays a landward-deepening bathymetric profile (De Santis et al. 1999) that is typical many areas around the Antarctic continental margin (Cooper et al. 1991a). In the Ross Sea, the profile is attributable to the effects of many cycles of ice sheet grounding line and retreat (ten Brink et al. 1997).

An unconformity named RSU-6 overlaps and cuts across the faults and seismic-sedimentary layering of the lower RSS-1 (Brancolini et al. 1995). The unconformity bevels the lower stratal package and is overlain by laterally continuous, flat lying, undisturbed reflectors considered to be of late Oligocene-early Miocene age (RSS2, Luyendyk et al. 2001, Sorlien et al. 2007). Age control of ca. 25 Ma is provided by microfossil identification from the upper RSS2 at DSDP site 270. Undeformed, laterally continuous glaciomarine deposits, including ice front features such as deltas and moraines occur in the RSS2 (De Santis et al. 1999, Sorlien et al. 2007). Unconformities dip northward

and the seismic sequences downlap to the north. The Central Trough and Eastern Basin contain several kilometers of Oligocene sediments, interpreted as deposits accumulated during extension and subsidence that mark an end to the sediment-poor conditions of the Paleogene (Decesari et al. 2007). Approximately 40 km of extension was distributed across the Central and Eastern basins, compared to 95 km of extension accommodated by the Northern and Victoria Land Basins in the western Ross Sea (Cande et al. 2000, Granot et al. 2013).

Counter to expectations, broad positive Bouger gravity anomalies (wavelengths of 100–200 km) in the Ross Sea and interior West Antarctica exist over the sedimentary basins and negative anomalies occur over the basement highs (Karner et al. 2005, Bell et al. 2006). Shallow magnetic anomalies over the shallow basement highs alternate with deep magnetic anomalies at >3800 m depth that are associated with the broad basins (Bell et al. 2006), and likely are attributable to mafic igneous rocks or thinned crust (Tréhu et al. 1993). Small circular shallow magnetic anomalies perturb the broad basin anomalies; these are attributed to small volcanic centers. This perplexing inverse density relationship for depocenters potentially arose as a result of flexural rigidity imparted during a period of slow/low sedimentation during lithospheric cooling following rifting (Karner et al. 2005) between the Eocene to Miocene (Wilson et al. 1998, Cape Roberts Science Team 2000, Hamilton et al. 2001, Luyendyk et al. 2001).

Within the WARS, active Cenozoic extension and alkali volcanism is ongoing in the Terror rift (Fig. 3-14), within the Victoria Land Basin at the western limit of the Ross Sea, bordering the Transantarctic Mountains (Fielding et al. 2008). The narrow zone of active extension and magmatism is kinematically linked to Eocene-Oligocene oceanic spreading across the Adare Trough to the north, within the oceanic portion of the Antarctic plate (Cande et al. 2000, Davey et al. 2006). Extension of ~150 km has occurred across the Terror rift (Stock & Cande 2002, Davey et al. 2006, Granot et al. 2010, Granot et al. 2013). Rift-related alkaline magmatism began at ca. 50 Ma along the west boundary of the West Antarctic rift province (Rocchi et al. 2002), and at ca. 28 Ma in Marie Byrd Land (LeMasurier et al. 2011), and magmatism continues today. In central Marie Byrd Land, polygenetic volcanism began at ca. 14 Ma, and a chronology of volcanism from the Miocene to Recent is well known (e.g. Wilch et al. 1999, Wilch & McIntosh 2002, Rocchi et al. 2006). Volcanoes of 19 to 6 Ma age form north-south chains, whereas volcanoes younger than ca. 6 Ma are distributed along east-west trends.

Oligocene to Present kinematic and geodynamic models predict active tectonism in central and eastern West Antarctica, also (Müller et al. 2007, Croon et al. 2008, Granot et al. 2013), particularly through fault reactivation (Müller et al. 2007, Paulsen & Wilson 2010). Resolution of structures is low due to the presence of the West Antarctic Ice Sheet. Despite this, there is considerable evidence of the dynamic state from bed topographic and geophysical datasets, including: narrow, deep troughs inferred to be controlled by faults (e.g. Jordan et al. 2010, Bingham et al. 2012); Cenozoic magmatism (Behrendt et al. 1996) and young volcanism (Wilch et al. 1999, Gaffney & Siddoway 2007, Corr & Vaughan 2008, Lough et al. 2013); rapid exhumation of Cenozoic intrusive rocks to the surface (Rocchi et al. 2006); and a high geothermal flux ~~high flux~~ of 115 mW/m², locally reaching 200 mW/m² (Maule et al. 2005, Schroeder et al. 2014, Dziadek et al. 2017, Wiens et al. 2013).

The Miocene and younger polygenetic volcanoes form elongate vents and volcanic edifices have a shape anisotropy (alignment, elongate shape, and vent distributions) that is interpretable in terms of a maximum horizontal strain orientation, which in turn reveals the Neogene state of stress across West Antarctica (Paulsen & Wilson 2010). The

orientation of the maximum horizontal stress direction based on the elongate orientation of post-6 Ma volcanic centers is oriented east–west (Paulsen & Wilson 2010), which is parallel to the absolute motion of the Antarctic plate (Müller et al. 2007, Croon et al. 2008). This geodynamic framework makes the preexisting tectonic boundaries between the Marie Byrd Land, Thurston Island/Eights Coast, and the Ellsworth-Whitmore Mountains terranes susceptible to strike-slip reactivation (Dalziel 2006, Müller et al. 2007). Therefore, recent plate dynamic models attribute the profound depths of the Byrd Subglacial Basin and Bentley Subglacial Trench (Fig. 3-1) to tectonic activity upon tensional structures or strike-slip releasing bends along a branch of the Cenozoic West Antarctic rift (Müller et al. 2007, Gohl et al. 2013a, b). Fault reactivation and potentially related processes such as geothermal activity or volcanism are of consequence because they may influence the dynamic behavior of the ice streams that have localized upon the terrane boundaries (e.g. Holt et al. 2006, Gohl et al. 2013a, Schroeder et al. 2014).

Continental shelf sediments

The rifted margin of West Antarctica is conjugate to the Chatham Rise (Fig. 3-6), formed as a result of separation between Zealandia and West Antarctica, circa 87 Ma ago. This contrasts with the active margin in the Antarctic Peninsula, where subduction continued until the Antarctic–Phoenix spreading ridge migrated into the trench (Larter et al. 2002; Eagles et al. 2004). Sediment thicknesses on the shelf have been calculated using multi-channel seismic reflection, swath bathymetry, borehole, and gravity modeling data. The sediment volume along the West Antarctic margin exceeds 3 million km³ (Wilson et al. 2012, ANTOSTRAT 1995), and may be as great as 10 million km³ (Wobbe et al. 2014, and references therein). Wobbe et al. (2014) estimate that 2.78 million km³ of sediment reside in the Ross Sea basin, with the remainder positioned in the Amundsen Sea and Bellingshausen Sea basins along the continent-ocean boundary (Fig. 3-13). Much of the sediment is of glaciofluvial origins. The first big Antarctic ice sheets initiated at the Eocene–Oligocene boundary, at ca. 34 Ma, when there was a transition from greenhouse to icehouse climate conditions in Antarctica (Zachos & Kump 2005, and references therein). Continental glaciation initiated, according to numerical models, in elevated areas of the West Antarctica terranes, followed by outward growth to form ice sheets (e.g. DeConto & Pollard 2003, Pollard & DeConto 2009).

The shelf and slope sequences of the outer shelf and upper slope, revealed by multi-channel seismic reflection and swath bathymetry (Nitsche et al. 2000, Nitsche et al. 2007, Lowe & Anderson 2002), are a product of glacial transport and sedimentation since the Oligocene (cf. Rocchi et al. 2006, Sorlien et al. 2007) or after. Lower aggradational sequences formed in a glacial marine environment when the West Antarctic ice sheet was of reduced extent on the inner shelf. Upper progradational sequences indicate the presence of grounded ice sheets of maximum extent that reached the shelf edge (Nitsche et al. 2000).

Wilson et al. (2012) use seismic stratigraphic records from ANTOSTRAT (1995) for Ross Sea sediment volume, and Nitsche et al. (2000, 2007), Scheuer et al. (2006), and Gohl et al. (2013b) for coastal eastern MBL, to calculate minimum and maximum bounds on the amount of crustal material from continental West Antarctica that must have been eroded to form the Oligocene and younger marine sediments that accumulated in the Ross Sea and on the Amundsen-Bellingshausen continental margins. There is an observed volume of 3.1 to 5.6 million cubic kilometres of sediment in these depocenters, that

corresponds to a source volume of 2.05 to 4.94 million km³ in ‘onshore’ West Antarctica. Wilson et al. (2012) used the estimated volumes of material eroded from the interior source regions to reconstruct a plausible Eocene-Oligocene paleogeography for West Antarctica. The restoration of the large volume of eroded sediments (that now reside on the shelf) to their prior position on land yields a reconstructed paleogeography with elevations ranging from present-day sea level up to a few hundred meters in elevation. The presence of upland areas during a time of cooling of global climate potentially influenced the growth of the first continental ice sheets (Wilson et al. 2012, cf. Pollard & DeConto 2009).

3.6.4. Characteristics and origin of the Marie Byrd Land volcanic province

Cenozoic volcanism in Marie Byrd Land occurs along a distance of nearly 1000 km along the northern edge of the West Antarctic rift province (Fig. 3-16). Alkaline volcanism in this province initiated at circa 30 Ma and continued through Quaternary time (Hart et al. 1995, Hart et al. 1997, Hole & LeMasurier 1994, Wilch et al. 1999, Wörner

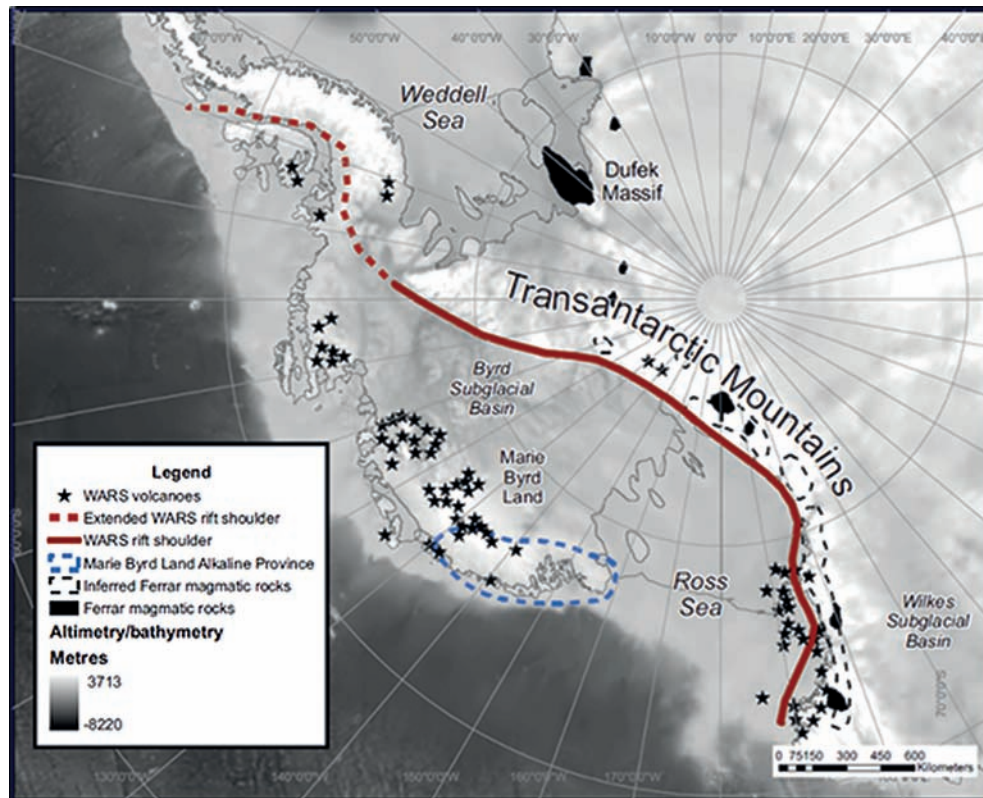


Fig. 3-16. Map of the West Antarctic Rift province from Storey et al. (2013), with location of Cenozoic alkaline volcanic centers indicated by star symbols. The outline of the extent Middle Jurassic Ferrar magmatism is shown with the dashed line symbol, and large Jurassic magmatic centers are shown in black. The region affected by mid Cretaceous alkaline magmatism in Marie Byrd Land is delimited with a dashed line in grey.

1999, LeMasurier & Rocchi 2005, Rocchi et al. 2006, Storey et al. 2013). Eighteen large alkaline volcanoes that attain circa 3000m elevation consist of dominant felsic alkaline lavas, phonolite, trachyte, and intermediate differentiates. Upon these volcanoes, parasitic vents produced scoria and lava flows made up of alkali basalt, hawaiite, and basanite. There is high interest in the geochemistry, history and time scales of volcanism due to recognition of Late Pleistocene to Holocene explosive tephra eruptions from four >3000m volcanoes spaced along the length of the volcanic province (Wilch et al. 1999). There have been recent discoveries of basaltic tephra from a large eruption at circa 2.2 ka that blanketed an area of 23,000 km² (Corr & Vaughan 2008), and of small-magnitude, long-period earthquake swarms indicative of deep magma movement that may presage an eruption (Lough et al. 2013; see below). A large subglacial eruption could have enormous consequences for the West Antarctic ice sheet and its subglacial hydrological system, as a result of meltwater production, bed lubrication, and ice discharge to the ocean (Vogel & Tulaczyk 2006, Fricker et al. 2007, Nitsche et al. 2013).

Neogene to present alkalic volcanism

Many of the alkali volcanic centers in Marie Byrd Land erupt lavas that have Sr-Nd-Pb isotope and trace element compositions characteristic of the HIMU mantle reservoir of ocean island basalts (Panter et al. 1997, Panter et al. 2000, Handler et al. 2003, LeMasurier & Rocchi 2005, Gaffney & Siddoway 2007, LeMasurier et al. 2011). The abbreviation HIMU (Hanyu et al. 2011) refers to lavas with high μ , where $\mu = {}^{238}\text{U}/{}^{204}\text{Pb}$. Isotopic characteristics include low ϵNd ($\leq +4$), low ϵHf ($\leq +3$), and radiogenic Pb isotopes (${}^{206}\text{Pb}/{}^{204}\text{Pb} \geq 21.5$). The radiogenic Pb isotopes are a product of processes that fractionate U/Pb and Th/Pb significantly over a long period, as for example within subducted, altered, partially melted oceanic crust that is surrounded by and hybridizes with surrounding deep mantle (Hanyu et al. 2011) over a long time period (10^9 years), or via stepwise development may be generated from a shallower source with a high U/Pb ratio in a shorter period of time, ca. 10^8 years (Rocchi et al. 2002).

The majority of magmatism in Marie Byrd Land occurred from 19 Ma to present, and therefore volcanism occurred in the presence of the West Antarctic ice sheet (LeMasurier & Rocchi 2005). Only a single volcano, Mt. Petras, is known to have originated earlier, from 29–25 Ma. The easternmost basalt/trachyte volcano, Mt. Murphy (LeMasurier et al. 1994), is a magnificent shield edifice that is underlain by hydrovolcanic deposits, about 400 m thick, that record lava-ice-water interactions. Exposures of basement gneisses exist beneath the lavas, a rare occurrence in Marie Byrd Land (see Fig. 3-10). The hyaloclastites and pillow lavas, with interbedded tillite indicative of the subglacial environment, are succeeded by subaerial basalt flows reaching a thickness of 1000 m, followed by felsic flows up to 550 m thick that form the summit of Mt. Murphy.

The westernmost well-exposed basaltic lavas occur in the Fosdick Mountains, where basalt and basanite flows are circa 1.4 Ma (Gaffney & Siddoway 2007). The Fosdick Mountains lavas have overall incompatible element abundances consistent with the HIMU-type signature (Hanyu et al. 2011, cf. Finn et al. 2005) of ocean island basalts. Their Pb isotopic compositions, however, are not radiogenic enough to be considered a direct representation of the HIMU mantle source in the strict sense. Each of the three centers in fact have distinct Sr-Nd-Pb isotopic characteristics, suggesting that there are at least three source components to the west MBL lavas. The interpretation is borne out by the lack of homogeneity among spinel peridotite xenoliths entrained within the flows:

the xenoliths exhibit wide variation in mineral assemblages, rock fabric, deformation intensity, and deformation mechanisms (Chatzaras et al. 2013, Chatzaras et al. 2016), despite the spatial proximity of the deep-sourced but comparatively low volume flows (Gaffney & Siddoway 2007).

The central MBL volcanic province (Fig. 3-16) is made up of isolated volcanic mountains and volcanoes along chains that are controlled by bedrock structures (Fig. 3-17) (e.g. LeMasurier & Rocchi 2005), presumed to be inherited faults. A majority are polygenetic shield volcanoes constructed from subaerial flows of nepheline-normative

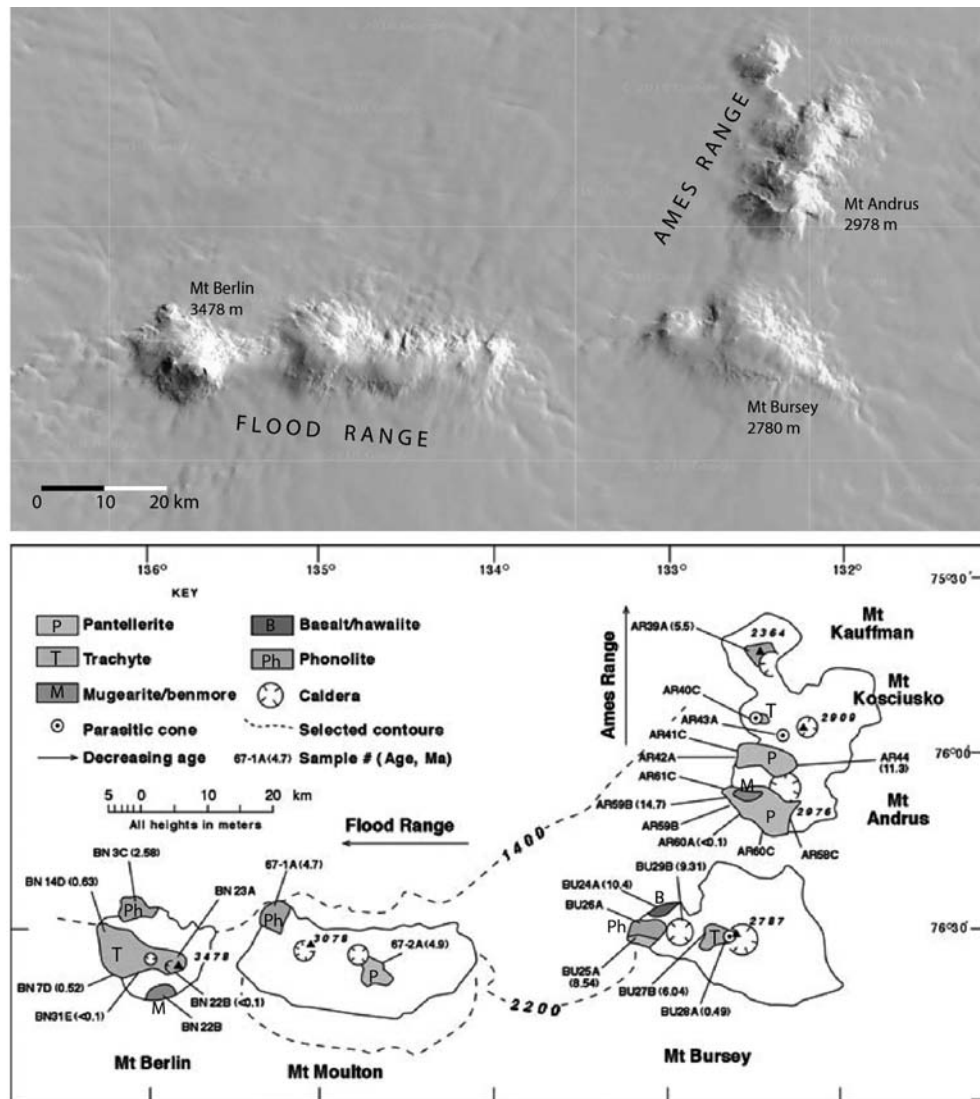


Fig. 3-17. (a) Satellite image of the Ames and Flood Ranges, sites of Miocene through Pliocene mafic alkali volcanism (GoogleEarth, DigitalGlobe, ©U.S. Geological Survey 2015b). (b) Sketch geologic map of the felsic and intermediate volcanic rocks at the crest of the Ames and Flood Ranges, from LeMasurier et al. (2011). Labeled sample localities show isotopic age information.

basanite and hawaiiite, hypersthene-olivine transitional basalts and trachytes, capped off by parasitic cinder cones and tephra of basanite containing nodules of spinel ilmenite, dunite, websterite, and other ultramafic xenoliths. An overall trend toward more felsic compositions from base to summit reflects magmatic differentiation in the centers over time, and is borne out by the late appearance of intermediate alkalic lavas (phonolite, which is an alkali feldspar – nepheline rock) and iron-rich, silica-poor rhyolite (pantellerite) in some centers (LeMasurier et al. 2011). The contemporaneity of the young magmas that differ strongly in composition potentially is a consequence of fractional crystallization over a long time period (LeMasurier et al. 2011).

Mount Sidley is a large polygenetic stratovolcano at the south end of the Executive Committee Range (Fig. 3-1). It consists of three major vent complexes that erupted phonolitic and trachytic lavas (Panter et al. 1997), with lesser pyroclastic rocks (Smellie et al. 1990). Phonolites were erupted between 5.7 and 4.2 Ma, giving way to trachytes at 4.6–4.5 Ma and small volumes of silica undersaturated lavas (benmoreite-mugearite series) at 4.4–4.3 Ma, along a southward compositional trend. Within Mt. Sidley, and along the Executive Committee Range as a whole, an apparent directionality to the petrological trends suggests south-directed pulses of volcanic activity attributable to tectonically driven or magma assisted fracture propagation (Panter et al. 1997). Sequential release of magmas due to progressive reactivation of an inherited structure may explain a perceived trend toward younger ages (Panter et al. 1994, LeMasurier & Rex 1989). New age and isotopic data do not support the radial age pattern (Paulsen & Wilson 2009).

New evidence for south-migrating magmatic activity along the trend of the Executive Committee range comes from two swarms of deep earthquakes in 2010 and 2011, recorded by the POLENET/ANET broadband seismic network (Lough et al. 2013). The swarms have unusual frequencies attributed to long-period seismicity, of a type that elsewhere in the world arises as a result of deep magma movements. The swarms are located beneath a subglacial topographic high, a positive magnetic anomaly, and an englacial mafic tephra layer. Taken together, the features point to the existence of a sub-ice volcano situated >55 km south of the southernmost exposure of volcanic rock in the area. An ancillary effect of magma migration in this sector could be elevated background heat flow beneath one of the West Antarctic ice streams. A possible significant consequence could be a subglacial volcanic eruption causing an outburst of glacial melt water in the ice streams' catchment (Lough et al. 2013).

Youngest eruptions across Marie Byrd Land (Wilch et al. 1999, Gaffney & Siddoway 2007) are dominated by peralkaline trachytes, with minor phonolites. These emanated from Mounts Takahe (Fig. 3-18), Berlin (2.7 Ma), Moulton, Siple, and small centers in the Fosdick Mountains in the Plio-Pleistocene. Volcanic products include agglutinated pyroclastic fall deposits containing pumice fragments, welded trachyte ignimbrite, welded autoclastic breccias, and lithic- and ash-rich explosion breccias containing volcanic bombs.

Mt. Siple, an isolated symmetrical volcano that rises from sea level along the Hobbs Coast (Fig. 3-1), has extensive ice cover and offers few exposures for petrological and geochronological investigation. Satellite cones around the base are basanite of <100 ka age. The caldera rim consists of pyroclastic fall deposits that are moderately to densely welded and yield an age of 227 ka. A subsidiary cone below the summit crater is 168 ka (Wilch et al. 1999). Mt. Takahe volcano to the east is, like Mt. Siple, a graceful, ice-shrouded, symmetrical volcano that is virtually undissected by erosion. Very limited exposures exist of lava alternating with densely welded pyroclastic rocks occur near the rim of the volcano's broad, low summit crater that is 8 km across (Wilch et al. 1999).

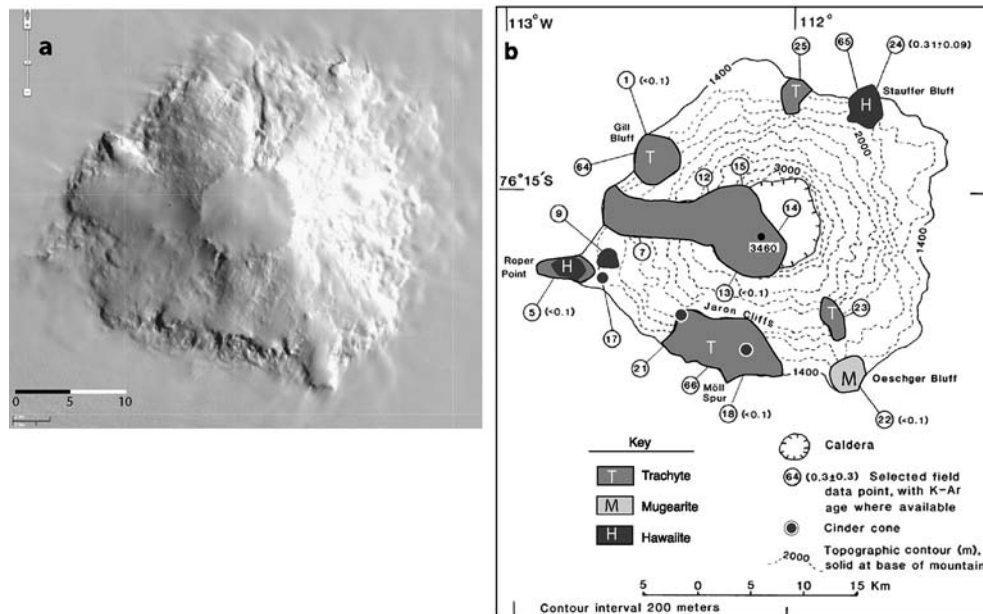


Fig. 3-18. (a) Satellite image of Mt. Takahe trachyte volcano, Pleistocene in age (GoogleEarth, Digital-Globe, ©U.S. Geological Survey 2015c). Diameter of crater is 8 km and base is ~30 km, with vertical relief ~2000 m. Trachytic compositions are characteristic of most exposures at Mt. Takahe, with subordinate mugearite and basanite/hawaiiite. (b) Geologic sketch map of Mt. Takahe, from LeMasurier (2013), showing trachyte and subordinate mugearite and basanite/hawaiiite. Labeled sample localities show isotopic age information.

$^{40}\text{Ar}/^{39}\text{Ar}$ dating of anorthoclase yields ages of 192 and 93 ka. The rim is composed of hydrovolcanic tuffs, obsidian-bearing bomb-and-block layers, welded to nonwelded pyroclastic lapilli deposits, and lavas that are just 8200 years old (Fig. 3-18).

The hydrovolcanic deposits are produced by lava – ice interactions on the Marie Byrd Land volcanoes. The preservation of these easily eroded deposits, on the upper slopes of >3000 m volcanoes, is due to the greater extent and height of the West Antarctic ice sheet during the Miocene to Holocene (Ackert et al. 1999, Wilch & McIntosh 2002, LeMasurier & Rocchi 2005). A superb example of lithofacies analysis of ice-contact versus subaerial eruption products in the Cray Mountains (Wilch & McIntosh 2002), documents a record of fluctuations between pillow lava and hyaloclastite breccia – indicative of wet, ice-contact conditions – and effusive lavas with welded breccia deposits, reflecting ‘dry’ subaerial environments. Sequences of this type are documented also at Mt. Murphy, 150 km away, where they are interrupted by erosion surfaces and intravolcanic tillites. The ages for the volcanic rocks are 9 to 6 Ma, and hydrovolcanic facies predominate between 9 and 8 Ma, based on $^{40}\text{Ar}/^{39}\text{Ar}$ geochronology, suggesting the a maximum extent of the ice sheet in the late Miocene (9.3–8.2 Ma BP) in eastern Marie Byrd Land (Mt. Murphy–Crary Mountains area; Wilch & McIntosh 2002). Hyaloclastic breccias of ca. 590 ± 15 Ma near the summit of Mt. Murphy, along the coast, indicate that the most recent ‘high stand’ of the WAIS was attained at 550 m above current levels.

Tectonic context for magmatism and relationship to West Antarctic Rift System

The origin of diffuse alkaline magmatism across West Antarctica, thermal and seismic anomalies in the mantle beneath the region, high topography in areas of thin crust, and relationship of magmatism to the rift province is much debated, and multiple viable hypotheses are in play (LeMasurier & Rex 1989, LeMasurier & Rex 1991, LeMasurier & Landis 1996, Finn et al. 2005, Sutherland et al. 2010, LeMasurier et al. 2011, Storey et al. 2013). A hypothesis for the presence of a mantle plume (LeMasurier & Rex 1989, LeMasurier & Rex 1991, Hole & LeMasurier 1994, LeMasurier & Landis 1996) or fossil mantle plume (Hart et al. 1997, Panter et al. 2000) beneath Marie Byrd Land has gained much traction, insofar as it potentially explains the trace elements and Sr-Nd-Pb isotopes pertaining to the HIMU-ocean island basalt characteristics, indicative of a primitive mantle source; the increase in elevation toward the interior of Marie Byrd Land; and a perceived radial, outward-younging age pattern for the trachytes. Advocates of a Cenozoic/active plume place the time of onset at ca. 30 Ma (e.g. Hole & LeMasurier 1994, LeMasurier & Landis 1996).

Relevant for the mantle plume hypothesis, an historic conception ~~has been~~ that the Antarctic tectonic plate ~~had~~ been stationary in respect to global plate tectonic circuit since 80 Ma (e.g. LeMasurier & Rex 1989, LeMasurier & Landis 1996), due to the dominance of divergent boundaries surrounding the plate. However that situation is now known to be false (Croon et al. 2008): contemporary models indicate the effects of integrated ‘ridge-push’ forces upon West Antarctica, that arise from the ridge-transform zones (Zoback 1992). Furthermore, the perceived outward-younging, radial age pattern for felsic volcanism in MBL (LeMasurier & Rex 1989) has been disproven by more comprehensive sampling and in-depth field study (Rocchi et al. 2002, Paulsen & Wilson 2010, Kipf et al. 2014).

~~One recent~~, alternative hypothesis attributes the alkali volcanism, mantle anomalies, and topographic effects (Fig. 3-16) to decompression melting of the mantle due to crustal thinning achieved by rifting (e.g. Wörner 1999) or wrench deformation (e.g. Rocchi et al. 2002). In this instance, the HIMU characteristics may be a relic of a Mesozoic plume that underplated the lithosphere (Weaver et al. 1994) prior to/during mid-Cretaceous rifting in the WARS and breakup of east Gondwana, rather than evidence of an active plume (e.g. Rocholl et al. 1995, Hart et al. 1997, Panter et al. 2000). A third hypothesis is for upward flow of enriched, lower density mantle above a zone of sinking of oceanic slabs introduced into the sublithospheric mantle during Paleozoic and Mesozoic subduction (Finn et al. 2005), with the possibility of mantle upwelling induced in response to cessation of Gondwana subduction (Sutherland et al. 2010). The compositional range of Marie Byrd Land lavas appears to reflect mixing between melts derived both from dehydrated oceanic crust and from subcontinental lithosphere metasomatized by fluids released from the slabs. Moreover, the residual, potassic, hydrous phases indicate more moderate temperatures in the mantle domains, that could produce “hot-spot-like” basalts without the need for a deep mantle plume. Such a scenario is consistent with the tectonic setting of MBL magmatism and the depth of the mantle anomaly, that is attributable to subduction of altered (hydrated) oceanic lithosphere beneath East Gondwana (West Antarctica) ~~occurred~~ over a long period of Paleozoic and Mesozoic time, leading to the release of fluids from the subducted slab(s) (Finn et al. 2005, Rocchi et al. 2002, Rocchi et al. 2006, Sutherland et al. 2010).

Finally, the elevated region is not circular, as typically is the case for mantle plumes, and centers of magmatism are distributed along linear rather than radial trends. Furthermore, the plume hypothesis does not explain the onset of magmatism in the middle Eocene. Valuable information about the intraplate stress state and the locus of volcanism comes from the orientation and alignment of Miocene to Holocene volcanic cones and vents in Marie Byrd Land provide (Paulsen & Wilson 2010). Elongation directions of volcanic vents, craters, and edifices reveal a maximum horizontal strain **direction** oriented north-south in early Miocene time. Younger volcanoes, <6 Ma in age, display a shape anisotropy that is orthogonal to that of Miocene volcanic centers, revealing that there has been a change in the maximum horizontal strain direction. Neogene plate motions produced north-south-oriented maximum horizontal strain in West Antarctica from the Late Miocene through Pliocene (~20 to 12 Ma;), when the Flood Range and Toney Mountain developed (LeMasurier & Rocchi 2005, Paulsen & Wilson 2010). From 6 Ma to present, the maximum horizontal strain has been oriented east-west during the time of construction of most of the Executive Committee Range, culminating with the eruption of Mt Waesche. The current standpoint is that the magmatism in the province is strongly localized along preexisting zones of weakness imparted during Paleozoic-Mesozoic convergence along the margin of East Gondwana and as a result of Cretaceous intracontinental extension (Finn et al. 2005, Rocchi et al. 2002, Rocchi et al. 2005, Paulsen & Wilson 2010, Kipf et al. 2014).

3.6.5. Paleotopography and landscape rejuvenation

The highest non-volcanic peaks in MBL are spaced over a wide region of outcrop in the Ford Ranges and Edward VII Peninsula (Fig. 3-6a), where summit elevations are between 700 and 1200 m (Stone et al. 2003). The remaining coastal nunataks and summits range in elevation from 150 to 600m, and emerged from beneath the West Antarctic Ice Sheet since Last Glacial Maximum (Stone et al. 2003, Sugden et al. 2005; Lisker & Olesch 1998, Lindow 2014, Spiegel et al. 2016). The low-lying topography and comparatively small range of bedrock elevations in coastal and western Marie Byrd Land precludes the use of thermochronology ‘elevation profiles,’ of the type that illuminate the Cenozoic landscape evolution of the Ellsworth and Transantarctic Mountains (Gleadow & Fitzgerald 1987, Fitzgerald & Stump 1991, Lisker 2002, Balestrieri & Bigazzi 2001).

As an alternative in MBL, valuable insights about age and exhumation history come from thermochronology data obtained over limited range of elevation and a broad coastal area (Fig. 3-12). Diverse isotopic systems including U-Pb zircon and Ti-in-zircon for igneous crystallization ages, U-Pb ages for growth of metamorphic monazite, $^{40}\text{Ar}/^{39}\text{Ar}$ for closure ages for multiple mineral systems, and apatite fission track and (U-Th)/He zircon cooling ages for migmatite and granite complexes (Richard et al. 1994, Mukasa & Dalziel 2000, Lisker & Olesch 1998, Siddoway et al. 2004b, Contreras et al. 2012, Lindow 2014, McFadden et al. 2015, Spiegel et al. 2016) all produce a consistent narrow range of ages from 102 to 88 Ma. Unimodal distribution of apatite fission track lengths of >13.4 μm indicate rapid translation through the apatite partial annealing zone (PAZ) (Lisker & Olesch 1998, Contreras et al. 2012).

The (U-Th)/He zircon and apatite fission track ages for fifteen non-volcanic summit locations all **yield of** 98 Ma to 88 Ma (Richard et al. 1994, Lisker & Olesch 1998, Contreras et al. 2012, Lindow 2014, Spiegel et al. 2016) that overlap with both U-Pb

igneous crystallization and $^{40}\text{Ar}/^{39}\text{Ar}$ mineral cooling ages of granite or migmatite from the same sites. The close correspondence between Cretaceous igneous crystallization ages and low temperature thermochronometers, and the narrow range of ages from the low temperature methods, provide evidence of very rapid cooling across the broad region due to tectonic exhumation during intracontinental extension (McFadden et al. 2015). Evidently, mid-crustal rocks that originated at $>700^\circ\text{C}$ at depths of 20 to 24 km at ca. 100 Ma passed through the $180\text{--}200^\circ\text{C}$ zone for partial retention of helium in zircon (Reiners 2005) and the $120\text{--}60^\circ\text{C}$ apatite partial annealing zone at depths <2 km (Kohn et al. 2005) by ca. 88 Ma. This likely was achieved by the tectonic translation of high temperature rocks to shallow depths upon regional-scale detachment faults (Fig. 3-12), including those that are well-documented at three locations in Marie Byrd Land and the Ross Sea (Fitzgerald & Baldwin 1997, Siddoway et al. 2004a, McFadden et al. 2010b). The tightly clustered older ages from summit elevations ($>800\text{m}$) potentially reflects the preservation of a ‘fossil’ apatite partial annealing zone (e.g. Toraman et al. 2014) as a result of slow cooling and very limited denudation after 88 Ma. The presence of a “fossil PAZ” is compatible with the preservation of a Cretaceous erosion surface in Marie Byrd Land (LeMasurier & Landis 1996) and the apparent lack of Moho relief beneath the Ford Ranges (Luyendyk et al. 2003).

Lower-elevation outcrops, <600 m above sea level, yield more scattered apatite fission-track and (U-Th)/He zircon ages, between 83–60 Ma (Richard et al. 1994, Lisker & Olesch 2003, Contreras et al. 2012, Spiegel et al. 2016). The low-elevation sites are coastal, or at the border of fast-flowing outlet glaciers, which are subject to change due to glacial loading/unloading, accommodated in part by small differential fault movements. The scattered younger ages and lack of interpretable pattern at elevations $<700\text{m}$ suggest that incision into the inferred “fossil PAZ” commenced somewhat recently and in an uneven manner (e.g. Toraman et al. 2014). Possible evidence for the onset of active glacial erosion into the regionally extensive crust that contains the imprint of anatexis and rapid cooling in the Cenomanian-Turonian Stage is the presence of detrital zircons of 110–100 Ma age within contemporary glacial sediments of Bindschadler and Kamb ice streams (Licht et al. 2014).

Evidence for the time of onset of erosional incision into a speculative “fossil PAZ” in West Antarctica in the Oligocene possibly is provided by widely separated sites at Mt. Murphy in eastern MBL and Roosevelt Island in western MBL. Mt. Murphy was discovered to be the site of rapid exhumation of an Oligocene gabbro from depths of 3 km or more (Rocchi et al. 2006), a finding that is corroborated by apatite fission track ages of 31 to 28 Ma from three sites (Spiegel et al. 2016). The exhumation or incision may mark the onset of growth of the elevated topography of the interior of Marie Byrd Land (i.e. “Marie Byrd Land dome”) since 30 Ma (Spiegel et al. 2016). In broadly contemporaneous strata on the opposite, western margin of Marie Byrd Land, deep, linear troughs are seismically imaged to incise pre-25 Ma sediments of the Roosevelt subbasin, bordering Edward VII Peninsula (Sorlien et al. 2007). The troughs clearly are sites of glacial incision and constitute the earliest evidence for landscape reactivation due to erosional incision in Marie Byrd Land Peninsula (Sorlien et al. 2007).

A broader distribution and denser sampling for thermochronology across MBL will be needed to verify the presence of a vestigial PAZ, and refine our understanding of the spatial-temporal evolution of topography in MBL. If achieved, the endeavor will help to clarify whether Miocene and younger bedrock incision occurs in response to dynamic support due to presence of warm mantle beneath MBL (LeMasurier & Landis 1996, Heeszel et al. 2016), onset of wet-based glaciation (Flower & Kennett 1994, Sugden et

al. 2005, Lindow 2014, Spiegel et al. 2016), or differential movement upon inherited faults due to change in the tectonic stress state (Rocchi et al. 2002, Rocchi et al. 2003a, Croon et al. 2008, Paulsen & Wilson 2010) and/or glacial unloading.

Pine Island Bay – Thwaites Glacier region

The tectonic boundary between MBL and Thurston Island/Eights Coast corresponds to the location of a north-south-oriented, deep, broad bedrock trough that underlies and extends inland from the Amundsen Sea Embayment. The Thwaites Glacier ice stream occupies this bedrock low (Fig. 3-1). A very narrow, deep, east-west oriented trough enters the Amundson Sea Embayment on the southeast, and is identified as an active rift (Jordan et al. 2010). This Pine Island rift forms the southern boundary of the Thurston Island block, and is occupied by Pine Island Glacier ice stream. The two ice streams together drain 4% of the outflow from the entire Antarctic Ice Sheet (Vaughan et al. 2006). The behavior of the ice streams is dynamically influenced by the geology and geomorphology of the subglacial bedrock, and is highly sensitive to warming of the ocean and atmosphere. The crustal thickness in this section is 19 ± 1 km based on the estimated Moho depth.

Bedrock geology and presence/absence of subglacial sediments are known to influence ice sheet behavior, in respect to the distribution of slow-moving sheet ice versus fast-moving ice streams. Across most of West Antarctica, the motion of the ice sheet is slow (Neumann et al. 2008) or stationary, where the ice sheet is fixed to the underlying bedrock (Bell et al. 1998). Crystalline bedrock (granitic rocks or migmatite gneiss; Kipf et al. 2012) or competent greenschist-metamorphosed siliciclastic rocks underlie such regions. Some evidence of the geology of the bedrock comes from the age distributions of detrital zircons obtained from subglacial sediments from the central to eastern ice streams; there is an age correspondence to bedrock sources in Marie Byrd Land, and no known sources in East Antarctica (e.g. Licht et al. 2014).

Elsewhere the ice sheet overlies sedimentary basin deposits or water-saturated till, materials that are porous and permeable, allowing the migration of water along and beneath the base of the ice sheet (Bell et al. 1998, Bell et al. 2006, Studinger et al. 2001, Fricker et al. 2007). Airborne geophysical surveys and ice drilling have shown that the fast-moving ice streams of West Antarctica, that flow several hundred meters per year, exploit zones where there are basal lubricants such as water or deformable till (Tulaczyk et al. 1998), that in some instances correspond with zones of higher heat flow. The margins of the fast-flowing ice correspond to high gradient anomalies that are interpreted as bedrock faults, an indication of bedrock structural control upon the locations for **streaming** ice (Studinger et al. 2001, Holt et al. 2006, Bingham et al. 2012).

The future outlook for the ice streams and West Antarctic ice sheet hinges on ice-bed dynamics. The ice streams that flow north toward the Amundsen Sea have beds below sea level that deepen toward the interior, a configuration that allows infiltration of seawater beneath the ice streams, allowing the seawater to infiltrate along the base, promoting streaming behaviour or flotation of the glacier ice, leading to grounding line retreat (Holt et al. 2006, Rignot et al. 2014).

A third geological element of the subglacial environment, identified on the basis of shallow-sourced magnetic anomalies that correlate with bed topography, is late Cenozoic volcanic rocks erupted from subaerial or subglacial centers (Behrendt et al. 2004, Behrendt 2013). Lavas erupted beneath and into the ice sheet would consist of

hyaloclastite, pillow breccia and other volcanic debris, that would be easily eroded by moving ice, whereas subaerial volcanoes, erupted during interglacial conditions, consist of more competent bedrock that forms higher-standing features. The subglacial volcanoes, together with crustal-scale structures that may influence the location of the centers of volcanism, are expected or documented (Blankenship et al. 1993, Blankenship et al. 2001, Schroeder et al. 2014) to be sites of high heat flow. Direct evidence of contrasts in the basal thermal regime and geological variations in the glacial substrate in Marie Byrd Land comes from landforms observed at upper versus lower elevations in recently deglaciated coastal regions (Sugden et al. 2005). Periglacial landforms at summit elevations (tors, well-developed granite grus) that form beneath cold-based ice are found in close proximity to glacially incised, scoured and sculpted bedrock that are produced beneath wet-based outlet glaciers at lower elevations along the coast.

3.7. Conclusion

The definition of the tectonic terranes of West Antarctica, achieved on the basis of direct field and laboratory investigations in geology, isotope geochemistry, and paleomagnetism, is being refined and expanded in the 21st century through the acquisition of network and grid geophysical and seismological/geodetic survey data (e.g. Wilson et al. 2011, Tinto et al. 2018). Variations in glacial bed topography, thickness of crust and whole-lithosphere, and mantle characteristics have been/are being modeled and mapped (e.g. An et al. 2016), to obtain a dynamic understanding of the lithospheric evolution of West Antarctica. The framework introduces new interdisciplinary questions about cryosphere-lithosphere interaction during a time of global change. Much new research focuses upon development of new continent-scale digital geological map resources with online access that encourages cross-discipline use (Cox et al. 2016), evaluation of the lithospheric scale structures that bound the terranes (e.g. Müller et al. 2007) and control the patterns of Neogene volcanism and heat flow (Paulsen & Wilson 2009, Fisher et al. 2015), and the discovery of the origin and consequences of anomalous mantle that underlies West Antarctica (e.g. Hansen et al. 2014).

